# PREDICTING THE DEPTH OF ANESTHESIA FOR OPERATING PATIENT USING MUSIC-BASED SPECTRAL FEATURES OF EEG SIGNALS

**M. N. NASHID RAHMAN**

**M. ENGINEERING PROJECT**

**DEPARTMENT OF BIOMEDICAL ENGINEERING**

**MILITARY INSTITUTE OF SCIENCE AND TECHNOLOGY**

**DHAKA, BANGLADESH**

**JANUARY 2023**

# PREDICTING THE DEPTH OF ANESTHESIA FOR OPERATING PATIENT USING MUSIC-BASED SPECTRAL FEATURES OF EEG SIGNALS

M. N. NASHID RAHMAN (SN: 0418260005)

A Project Submitted in Partial Fulfillment of the Requirement for the Degree of Master of Engineering in Electrical, Electronic and Communication Engineering

DEPARTMENT OF BIOMEDICAL ENGINEERING

MILITARY INSTITUTE OF SCIENCE AND TECHNOLOGY

DHAKA, BANGLADESH

JANUARY 2023

PREDICTING THE DEPTH OF ANESTHESIA FOR OPERATING PATIENT USING MUSIC-BASED SPECTRAL FEATURES OF EEG SIGNALS

M. Engineering Project

By

M. N. NASHID RAHMAN
(SN: 0418260005)

Approved as to style and content by the Board of Examination on 26 January 2023

| | | |
|---|---|---|
| 1. | Dr. Md. Asadur Rahman<br>Assistant Professor<br>Department of Biomedical Engineering<br>Military Institute of Science and Technology (MIST) | __________<br>Supervisor<br>(Chairman) |
| 2. | Col Syed Mahfuzur Rahman<br>Senior Instructor and the Head of the Department<br>Department of Biomedical Engineering<br>Military Institute of Science and Technology (MIST) | __________<br>Member<br>(Internal) |
| 3. | Dr. Md. Enamul Hoque<br>Professor<br>Department of Biomedical Engineering<br>Military Institute of Science and Technology (MIST) | __________<br>Member<br>(Internal) |
| 4. | Dr. Mohammad Shorif Uddin<br>Professor<br>Department of Computer Science and Engineering<br>Jahangirnagar University | __________<br>Member<br>(External) |

Department of Biomedical Engineering, MIST, Dhaka

PREDICTING THE DEPTH OF ANESTHESIA FOR OPERATING PATIENT USING MUSIC-BASED SPECTRAL FEATURES OF EEG SIGNALS

## DECLARATION

I hereby declare that this project entitled "***Predicting the Depth of Anesthesia for operating Patient Using MUSIC-Based Spectral Features of EEG Signals***" is my original work and has been written by me. Furthermore, I have duly acknowledges all the sources of information used in the project. This project has also not been submitted for any degree in any other university before.

____________________________

M. N. NASHID RAHMAN
0418260005

January 2023
Department of Biomedical Engineering, MIST, Dhaka

ABSTRACT

**PREDICTING THE DEPTH OF ANESTHESIA FOR OPERATING PATIENT USING MUSIC-BASED SPECTRAL FEATURES OF EEG SIGNALS**

In modern practice of major surgery using anesthesia is entirely mandatory. But due to the failure of optimal dose of anesthetic dose delivery it is also common to the patients to face intraoperative and postoperative complications. The main cause of the imbalance dose of anesthesia is not being sure to assess the depth of sleep of the patient or the depth of anesthesia or. Therefore, precise prediction of the depth of anesthesia or the proper assessment of transitional sleep state (from deep sleep to awake) could be a way out to set the optimal anesthetic dose by the anesthesiologist. In this work, a different approach of feature extraction and classification method is proposed to predict three different sleep states during surgery from the EEG signal. This work used an open-source database containing the EEG data of anesthetic patients during surgery. The data were separated into three states: into the deep-sleep state (IntoDeep), the deep-sleep state (InDeep), and the awake state (InAwake). The raw EEG signals were filtered and their power spectral (PSD) densities were calculated using MUSIC (multiple signal classification) model, a parametric method. These MUSIC based PSD values are taken as the features of the EEG signal. An artificial neural network model was trained to develop a machine learning based predictive model with the MUSIC based PSD features. Finally, the predictive model was verified by the data separated for testing and evaluated the prediction accuracy in subject-dependent and subject-independent approach. Eventually, it is found that the results are better than the existing works those worked on the same dataset.

**Key Words:** Anesthetic Depth; Electroencephalogram (EEG); Multiple Signal Classification (MUSIC); Artificial Neural Network (ANN).

# সারসংক্ষেপ

## PREDICTING THE DEPTH OF ANESTHESIA FOR OPERATING PATIENT USING MUSIC-BASED SPECTRAL FEATURES OF EEG SIGNALS

অস্ত্রপচারের সময় অ্যানেস্থেসিয়ার ব্যবহার এখন শর্তহীনভাবে বাধ্যতামূলক, যদিও এই অ্যানেস্থেসিয়া প্রয়োগের কারনে রুগীকে অস্ত্রপচারের আগে ও পরে বেশ কিছু ঝামেলায় পড়তে হয়। এটির অন্যতম কারন হল অ্যানেস্থেসিয়ার যথাযথ মাত্রা নির্ধারন করতে না পারা বা রুগী অ্যানেস্থেসিয়া প্রয়োগে ঘুমের কোন স্তরে অবস্থান করছে সেটা পরিমাপ করতে না পারা। এইজন্য, রোগী অ্যানেস্থেসিয়া প্রয়োগে ঘুমের কোন স্তরে অবস্থান করছে বা ঘুম থেকে জেগে উঠতে যাচ্ছে কি না তা পূর্ব থেকেই অনুমান করতে পারলে অপ্রয়োজনীয় চেতনানাশক এজেন্টগুলির ব্যবহার কমানো যেত। এধরনের কাজে সহযোগীতা করার জন্য আমরা মেশিন লার্নিং ভিত্তিক একটি মডেল প্রস্তাব করেছি যা EEG সংকেত থেকে অস্ত্রপচারের সময়কার তিনটি ভিন্ন স্তরের ঘুমের অবস্থার পূর্বাভাস দিতে পারে। এ মডেল তৈরীতে অস্ত্রপচারের সময়কার অচেতন করা রোগীদের EEG ডেটাসহ একটি ওপেন-সোর্স ডাটাবেজ সংগ্রহ করা হয়েছিল। সেই ডাটাটি তিনটি ভিন্ন অবস্থায় ভাগ করা হয়েছিল: গভীর ঘুমের দিকে যাওয়ার পূর্বাবস্থা (IntoDeep), গভীরভাবে ঘুমন্ত অবস্থা (InDeep), এবং গভীর ঘুম থেকে জেগে ওঠার অবস্থা (IntoAwake)। প্রথমে ডাটাবেসের এলোমেলো EEG ডাটাগুলিকে যথাযথ ফিল্টার করা হয়েছে এবং বিভক্তকৃত ডাটাগুলির স্পেক্ট্রাল ঘনত্ব (PSD) বের করা হয়েছে (MUSIC: Multile Signal Classification) মডেল ব্যবহার করে যেটি একটি প্যারামেট্রিক পদ্ধতি। এই MUSIC মডেল দ্বারা বের করা PSD এর মানগুলিকে সিগনালের বৈশিষ্ট্য (Feature) হিসেবে বিবেচনা করা হয়েছে। এরপর উক্ত সিগনালের বৈশিষ্ট্য সম্পন্ন ডাটাগুলি দিয়ে একটি কৃত্রিম নিউরাল নেটওয়ার্ক মডেলকে প্রশিক্ষন (Training) দিয়ে মেশিন-লার্নিক ভিত্তিক একটি অনুমানকারী মডেল (Predicting Model) তৈরী করা হয়েছে এবং তার কার্যকারিতা যাচাই (Validation) করা হয়েছে। অবশেষে, সেই মডেলটি ব্যবহার করে এর পরীক্ষন ডাটার (Testing Data) উপর এর কার্যকারিতা পরীক্ষা করা হয় এবং তার ফলাফল (সঠিকতা এবং ভুল করার প্রবনতা) গনণা করা হয়। প্রাপ্ত ফলাফলগুলিকে বিদ্যমান অন্য গবেষণার (যারা ঠিক এই ডাটাসেট নিয়েই গবেষণা করেছে) ফলাফলের সাথে তুলনা করে দেখা গেছে আমাদের প্রস্তাবিত কাজের ফলাফল অন্যদের থেকে উত্তম।

# ACKNOWLEDGEMENTS

At First, I would like to thank the most gracious and merciful Almighty Allah for showering the blessings and guidance throughout my project work for pursuing the M. Engg. degree and for giving me the strength to complete this project, successfully.

Then we would like to acknowledge my deep gratitude to the oral examination committee members and their guidance truly helped me to enhance the quality of this dissertation writing.

It is an immense pleasure to convey my sincere and deepest gratitude towards my supervisor, **Dr. Md. Asadur Rahman,** Assistant Professor, Department of Biomedical Engineering, MIST, thanks to him for his invaluable guidance, suggestions, energy, patience, and inspiration. This thesis would never have been done without his help and dedication at every step of this journey. Each meeting has been a wealth of information, and I have had a great time learning new things. To express my gratitude for his unfailing support, my supervisor deserves another word of thanks.

I would like to offer my special thanks to the respected Head of the Department, **Colonel Syed Mahfuzur Rahman**, for providing guidance and support. I must acknowledge the guidelines of **Prof. Dr. Md. Enamul Hoque** of BME department to improve the writing this dissertation. I would like to express my gratitude to all faculty members of the Department of Biomedical Engineering, MIST for their unwavering support and assistance during this project. I would also express my gratitude to other office staffs for their help.

Finally, I must acknowledge the support of my family members, especially my parents **Dr. Zillur Rahman** and **Dr. Nazmun Nahar**. Thank you dear wife **Dr. Rubaiyat Rashid** and my loving son **Md. Rishad Rahman Rehan** for your continuous sufferings and support during this journey.

Author

## TABLE OF CONTENTS

## LIST OF FIGURES

## LIST OF TABLES

## LIST OF ABBREVIATIONS

| | |
|---|---|
| ANN | Artificial Neural Network |
| ASA | American Society of Anaesthesiologists |
| $BIS^{TM}$ | Bispectral Index TM |
| CNN | Convolutional Neural Network |
| DFT | Discrete Fourier Transform |
| DoA | Depth of Anesthesia |
| ECG | Electrocardiography |
| EEG | Electroencephalogram |
| EMD | Empirical Mode Decomposition |
| FFT | Fast Fourier Transform |
| FIR | Finite Impulse Response |
| GA | General Anesthesia |
| LM | Levenberg-Marquardt |
| MUSIC | Multiple Signal Classification) |
| PSD | Power Spectral Density |
| WHO | World Health Organization |

# CHAPTER 1

# INTRODUCTION

## 1.1 Background

Anesthesia is an important prerequisite medication process before and during surgery to alleviate the pain of the patients. The drugs or medicines used for anesthesia are called anesthetics. Anesthetics are provided to the patient's body by the means of injections, eye drops, topical lotions, inhalation, sprays, skin patches, etc. Anesthesia is divided into three major categories: *i*) Local Anesthesia, *ii*) Regional Anesthesia, and *iii*) General Anesthesia (GA). Among these categories, GA plays the most vital role in critical surgeries (Vutskits, 2016). General anesthesia reduces brain’s activity, especially of the central nervous system, which makes the patient unconscious and the patient do not feel anything during the surgery. It can be done with either injected or inhaled drugs. It's usually performed in an operating room to allow surgical procedures that would be too painful for a patient or in an intensive care unit or emergency room. GA provides the following features to the patients: *i*) Unconsciousness (Lack of awareness and recall), *ii*) Analgesia (the inability to feel pain), and *iii*) Immobility (Lack of movement).

Nonetheless, this procedure (General anesthesia) often creates complications due to over-sedation or under-sedation of the anesthetics. Due to the over-sedation following post-operative complications may arise a longer wake-up time, Delirium, Cognitive dysfunction, Heart disease, Stroke, etc. (Gottschalk, 2011) .On the other hand, under sedation may create a situation when the patient’s awareness may arise (Cascella M. B., 2020). In this state, patients reminded the conversations of the doctors, even traumatic memories. Patients may gain unexpected anxiety for this type of knowledge that leads to serious post-traumatic stress disorder. A study (Heggy, 2020) collected data from 200 anesthetic patients those had the unpleasant memory related to his/her surgeries or GA. Sixty three (63) patients experienced no unlikely events but the remaining 137 experienced something unpleasant. The statistics of the different complications are summarized in **Figure 1.1**. Therefore, in clinical practice, always the optimal dose of anesthetics is a cherished demand, although it is always difficult to set the optimal dose level for patients of different diseases, ages, sex, health conditions, weight, previous complications, etc.

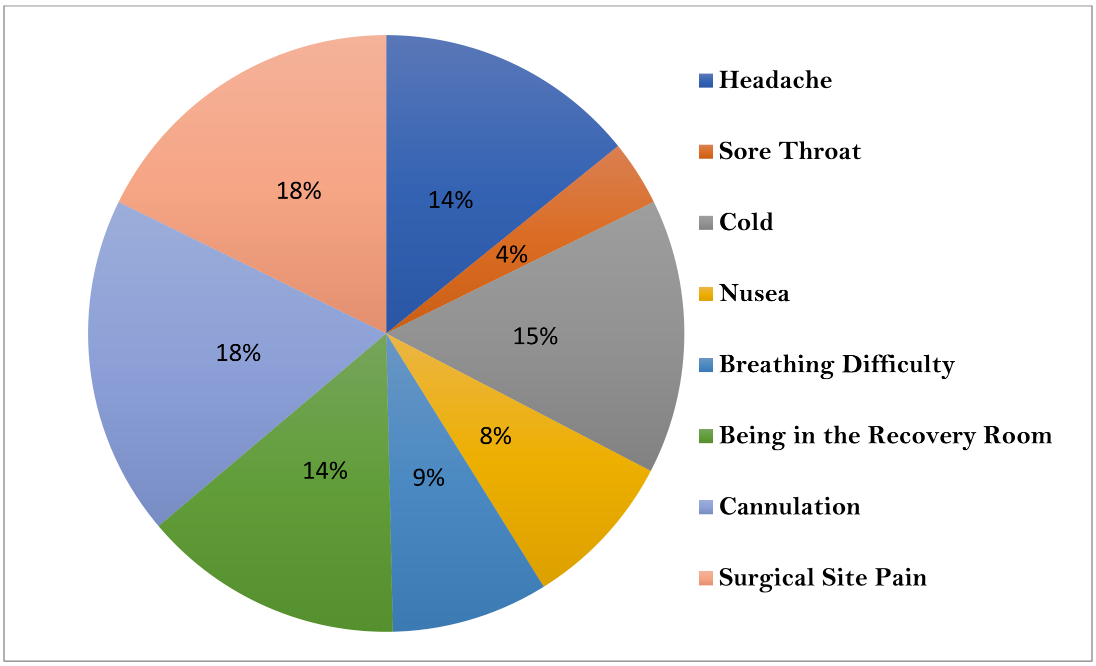


**Figure 1.1:** Patients recall unpleasant episodes related to surgery and anesthesia.

Anesthetics primarily work by increasing inhibitory cell activity while reducing excitatory cell activity. The ubiquitous receptors gamma-aminobutyric acid and N-methyl-Daspartate are commonly triggered by propofol, sevoflurane, and ketamine medications. During the loss of consciousness, generally it is observed that the communication between the neuron cells inside the brain is disrupted. Anesthetic agents alter the typical information processing mechanism inside the brain (Uhrig, 2014).

In general practice in clinic, major signs are utilized to determine the amount of anesthesia or depth of anesthesia (DoA). Because they may be influenced by variables unrelated to an aesthetic depth, these measures are unreliable markers of anesthetic adequacy. Pulmonary Cardiovascular measures are one of them and they include heart rate, mean arterial pressure, systolic/diastolic blood pressure, blood oxygen level, and respiratory rate). Some other clinical signs are also considered such as sweat, limb movement, and shedding of tears those are not reliable methods to determine the state of brain functionality during surgery (Rani, 2012). Therefore, direct monitoring the brain functionality could be the obvious solution to measure the sedation (Alsafy, 2022).

Several research studies (Alsafy, 2022; Madanu, 2021; Liu, 2018) suggested that the change in the scalp electrical potential in the region of frontal brain, i.e., measured as electroencephalogram (EEG), is directly correlated with the effect of GA. The functional interaction mechanism of central nervous system is conducted by the transmission and reception of neurons' action potential, which is the main mechanism for the processing of the brain information. This resulting functional activity affects the neuronal behavior, such as the firing rate, which can be assessed by the pattern of EEG. This is how the EEG behavior is closely related with different DoA levels (Liu, 2018; Shalbaf, 2015). Therefore, based on the aforementioned research works, it can be culminated that continuous brain function monitoring must be used for the prediction of the DoA. This method can prevent overdose of GA and ensure that patient's quick recovery from deep sleep avoiding the possible postoperative difficulties.

As a result, several EEG-based monitoring systems of DoA-level machines are developed (Poorun, 2016; McKeever, 2014; Shi, 2023). Previous research works proposed different features of frequency domain such as median frequency, power spectral density (PSD), spectrogram, spectral entropy, etc. with the bispectral index of EEG to envisage the DoA (Rogobete, 2021; Liu, 2018; Akeju, 2014; Carillion, 2015). Recent studies employed different machine-learning-based models to identify the DoA levels like group sparse-based model, recurrent neural network, hidden Markov models, etc. (Höcker, 2010; Gottschalk, 2011; Musizza, 2010).

## 1.2 Problem Statement

From current research works it is found that these researchers tried to find the consistent features of EEG signal during different depth of anesthesia. Some researchers took other physiological signals added to EEG signals to take decision on anesthetic depth. Only two research works so far those worked to find the prediction accuracy of two sleep sates: deep sleep and awake state. The first one (Madanu, 2021) used convolutional neural network to model a deep learning-based predictor to predict the anesthetic depth of two classes. This work avoided to extract features from the signal and took all signals to take decision by the deep learning model. On the other hand, the work described by (Rahman, 2022) calculated the signal's PSD of different band and find the band-wise sleep state prediction accuracy using a machine learning model trained by the PSD features from two classes. In this work, they used non-parametric Welch method to extract the PSD. Recent work (Hossain, 2023) states that parametric method especially MUSIC (**mu**ltiple **si**gnal **c**lassification) method is better in PSD estimation from the EEG signal. He also recommended to using MUSIC method with proper order selection in PSD selection, otherwise this estimation may not be effective to achieve target of feature extraction. Therefore, feature extraction from PSD and selection the proper order of parametric method are two factors of this work to take them as challenge to achieve the sole objectives of this work.

## 1.3 Objectives

The main objectives of this project:

- To extract the spectral features using MUSIC and predict the different levels of DoA
- To compare the accuracy of the proposed model with existing methods

## 1.4 Work in brief of this Project

This project employed a MUSIC-based parametric power spectral estimation mechanism to find the PSD of the EEG signal. The values of the MUSIC-based PSD were considered the features of the EEG signal of different DoA. The EEG signals of surgery patients were divided into three greater parts: (*i*) IntoDeep state, (*iii*) InDeep state, and (*ii*) IntoAwake state. The PSD of the EEG signal is extracted using suitable order. The extracted features were utilized for training the artificial neural network (ANN) to construct a machine learning-based predictive model. That model was also validated and tested for the testing dataset. Furthermore, the prediction accuracies of those three states were calculated as a subject-dependent and subject-independent approach. The results are compared with the other works that used the same dataset and found that the result of this project is better than the available works. Detail of this methodological chronology is described in Chapter 3.

### 1.5 Outlines

**Chapter 1 (Introduction)**: The introductory information like study background, project's problem statement and objectives, brief work description of this project are included in this chapter.

**Chapter 2 (Literature Review)**: The related literatures are widely discussed in this chapter with their speciality and limitations. Also this chapter indicates the logic of upcoming methodology followed by this proposal.

**Chapter 3 (Methodology)**: All small signal processing steps on the materials are mathematically and graphically explained with examples in this chapter. This chapter is the backbone of logics that are applied in the contextual data materials to get the results for achieving the objectives of this project.

**Chapter 4 (Results and Discussions)**: The results are presented in this chapter. Each small signal processing steps and corresponding outcomes from the dataset are discussed here with graphical plots, numerical tables, comparison tables, etc.

**Chapter 5 (Conclusions):** Whole work with its effectiveness and limitations are concluded in this chapter. Also, feature perspective is added in this chapter.

# CHAPTER 2

# LITERATURE REVIEW

Anesthesia is one of the most important steps in surgery and monitoring continuously its consequence which is termed as DoA. It is still a challenge for the clinical practitioners and researchers to monitor the DoA. Predicting the depth of anesthetic levels during surgery helps the doctors to provide exact dose to the patients and benefits the patients from the side effects of the anesthetic overdose of the Traditional monitoring techniques rely on the patient's physiological response and skilled anesthesiologists. Relying on such methods might give erroneous results. WHO (World Health Organization) conducted a study (Gottschalk, 2011) and showed that the mortality due to surgical complications mostly caused by anesthesia overdose. Therefore monitoring this anesthetic depth or DoA during surgery is a significant concern for providing improved patient's care (Cascella, 2016).

To correlate the DoA and different factors related to patients physiological signals, considerable amount of research work has been carried out. One study proposed that the brain's electrical activity or electroencephalography (EEG) has a strong relationship with the transition of the different levels of anesthesia (Musizza, 2010). This EEG signal can be measured from the scalp of the patient during surgery noninvasively. In recent classification of DoA, EEG frequency spectrum has achieved expanded momentum due to having its different feature extraction methods. Although EEG-based methods cannot be declared as optimum method for DoA classification, recent research works regarding this area appears to be quite encouraging.

Since the change in the frequency of EEG signal correlates with different DoA, researchers adapted and deployed different analytical methods on the EEG signal to extract consistent features for understanding the DoA. These include the methods of time-frequency analysis like wavelet transform (Frasch, 2015), short time frequency transform and continuous wavelet transform (Kıymık, 2005). Nonlinear chaotic parameter based EEG signal analysis is also deployed considering this signal's nonlinear property (Lalitha, 2007), (Hutt, 2013)has utilized a linear model of neural population that can predict the propofol's concentration during anesthesia where power spectrum of EEG signal was considered as the feature of the signal.

Spatio-temporal patterns of EEG signal are analysed in (Zhang, 2001) using Lempel-Ziv analysis. Comparative effect analysis of different pattern recognition methods are widely studied and in (Amin, 2017) and different cognitive task are classified with the help of machine learning algorithm. The previous results in terms of the classification accuracy are compromised and inefficient to determine the internal changes for individual patient's characteristics.

Achieving high classification accuracy is always a tradeoff between time and computational complexity of feature extraction. Therefore, simple feature extraction method is always recommended for real-time signal processing and DoA monitoring. As EEG spectrum is associated with DoA, EEG signal power and PSD are most reliable features of EEG signal for predicting the levels of anesthetic depth. Most researchers used non-parametric methods like Welch or sliding window Welch method for estimating the PSD of EEG signal. There is a long debate regarding the issue of using the parametric and non-parametric PSD estimators. It is believed by all that the non-parametric method especially the Welch method is popular and straight forward technique to estimate the PSD of EEG signal but recently some work (Hossain, 2023) utilized parametric method MUSIC to estimate the PSD of EEG signal to extract the features for classifying the emotional state. In his work, he clarified that how MUSIC model extract the features from EEG signal taking less time than the Welch method as well as he achieved higher classification accuracy than the Welch method. Therefore, for real-time EEG signal analysis and DoA monitoring MUSIC model is a significant PSD estimation technique.

It is also mentionable that, there is only one publicly available dataset of EEG signal during surgery and the corresponding sleep state markers. Moreover, only two research works (Rahman, 2022) & (Madanu, 2021) are utilized this dataset and deployed their methods to classify the sleep states. (Madanu, 2021) used convolutional neural network (CNN) and empirical mode decomposition (EMD) method. In this method, using EMD, the EEG signals are decomposed upto 6-7 levels and after that these decomposed signals are used to create images. These images are feed in CNN model to extract features and classify the sleep states. This method is effective but time consuming and computationally inefficient. On the other hand, (Rahman, 2022) used Welch method to extract PSD of different EEG bands (alpha, beta, delta, theta, and gamma) and feed them in a simple multilayer perceptron neural network to classify the sleep sates. This method is computationally efficient but the classification accuracy is not up to the mark. Moreover, both these work considered two types sleep states: Awake and Deep sleep.

Therefore to overcome the current limitation of the available research work, in this project two hypothesis were set:

(*a*) EEG signal of DoA are to separate into three sleep states: *i*) IntoDeep *ii*) InDeep, and *iii*) IntoAwake.

(*b*) To estimate PSD of EEG signal MUSIC model is to be utilized

The utilized methods to overcome the limitations by following the aforementioned hypothesis are discussed in detail in the Chapter 3.

## CHAPTER 3

# METHODOLOGY

## 3.1 Introduction

From the previous research works, it is clear that prediction of three levels of DoA is challenging. Therefore most of the research works considered this as a two class (deep sleep and awake) prediction problem. This is a challenge of this proposed work to consider it as a three-class prediction problem and design associated methodology to achieve the acceptable prediction accuracy. Therefore, in this work parametric PSD was considered for feature extraction instead of non-parametric PSD such as Welch method. Besides, to predict the DoA levels there are some other signal processing steps. In this chapter, materials (dataset) and every processing step of the proposed methodology are discussed gradually.

## 3.2 Materials

### 3.2.1 Subjects

Prior to data acquisition of the medical patient to make this dataset, ethical approval was taken from the National Taiwan University Hospital and the proposed protocol of the data acquisition was granted by this hospital’s Research Ethics Committee under the ethical approval no 201302078RINC . All involved patients were informed verbally about the data recording and written consent was taken before their operations. In this study, only regular surgery under GA patients was considered for data acquisition. In addition, no patients were considered those who underwent high risk operations like the surgery of lung, heart, brain, etc. Alcoholic, smokers, and/or having other medical illness related that could affect data recording were excluded. Based on the previous selection criteria, 24 patients were finally accepted to make this dataset. Patients' metadata are following:

- Age: 44.5±12.9 years
- Height: 164.2±7.1 cm,
- Weight: 63.4±14.8 kg
- BMI: 23.4±4.2 kg/m$^2$,
- Gender: 14 females and 10 males
- Duration of the surgery: 126.4±72.9 min (from anaesthetic medical recording forms).

### 3.2.2 Anaesthetic Procedure Manipulation

The aesthetic procedure can be presented briefly as follows (Liu, 2018):

- **First:** The anaesthesiologists were informed about the Patients' clinical information like weight, height, gender, age, and type of operation to prepare anaesthetic plan.
- **Second:** It was confirmed that patients eat nothing for at least 8 h prior to the beginning of this study.
- **Third:** The obligatory procedures like routine and emergency drug check were conducted accordingly
- **Fourth:** A suitable volume of anaesthetic agents are then provided to each patient for the regular operations.
- **Finally:** The GA was confirmed by observing the other physiological signals such as EEG, ECG, pulse rate, blood pressure, heart rate, SpO2, etc.  These done by MP60 (Intellivue; Philips, Foster City, CA, USA). If any observed signal showed irregularity, the available doctors accustomed the intraoperative references anesthesia machine, accordingly.

Following anesthetic agents were provided to the patients according to the assessment of the anaesthesiologists: Propofol, Fentanyl, Atropine, Nimbex, Xylocaine, Maintenance Sevoflurane, Desflurane, Morphine, Ketamine, Atropine, and Vagostin. For understanding the whole process by a glimpse of illustration, a summary is given in **Figure 3.1**.

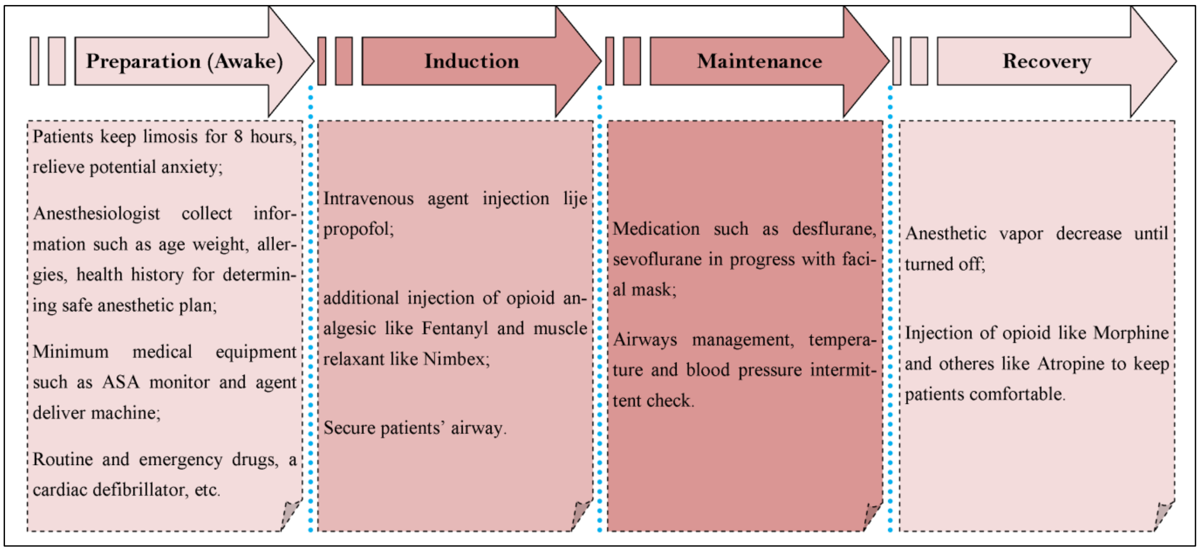


**Figure 3.1:** The conducted anaesthetic procedure in the used data recording. (ASA: American Society of Anaesthesiologists.)

### 3.2.3 Data Recording

The patients were prepared for EEG data recording by using a conductive paste between electrode and the frontal scalp skin to improve the conductivity (<5kΩ). The data recording was conducted by EEG BISTM Quatro Sensor (Aspect Medical Systems, Newton, MA, US). The EEG module was interconnected with MP60 machine through the connector cable prescribed by company. The raw EEG (continuous waveform) data were recorded on a laptop through the serial RS-232 with a sampling rate of 128 Hz.

## 3.3 Methods

### 3.3.1 Data Pre-processing

The clinical management and other physiological data were sorted accordingly. Then, the tasks like EEG data conversion, formatting, and event labelling were conducted. The EEG data of all patients (cases) were then visually scrutinized approximately to remove the precise sections of artefacts resulting in waveform inundation (e.g., noises or signal fluctuations caused by body movement or medical equipment), thus significantly decreasing the outlier point segments. A notch filter was used to remove the 60-Hz line noise. Up to this level of pre-processing was done previously by the team that acquired the data. Therefore, the dataset is pre-processed at a fringe level. This data needs a number of signal processing steps to attain the objectives of this project work. The major steps are given in the **Figure 3.2**.

In this project, after loading the dataset the data is processed further. All data are filtered with a band-pass filter considering the band is 0.3-45Hz. This band-pass filter was designed using an FIR (Finite Impulse Response) filter with hamming window of 100 orders. The characterized magnitude and phase diagram of such proposed FIR filter is shown in **Figure 3.3**. In this figure, the results (magnitude and phase) are shown with respect to the normalized frequency. Also, magnitudes are plotted in decibel (dB) unit. All patients' EEG signals were filtered using the designed window-based band-pass FIR filter where the band is considered as 0.3-45Hz. The filtering effect on signal is graphically presented in the Result and Discussion section.

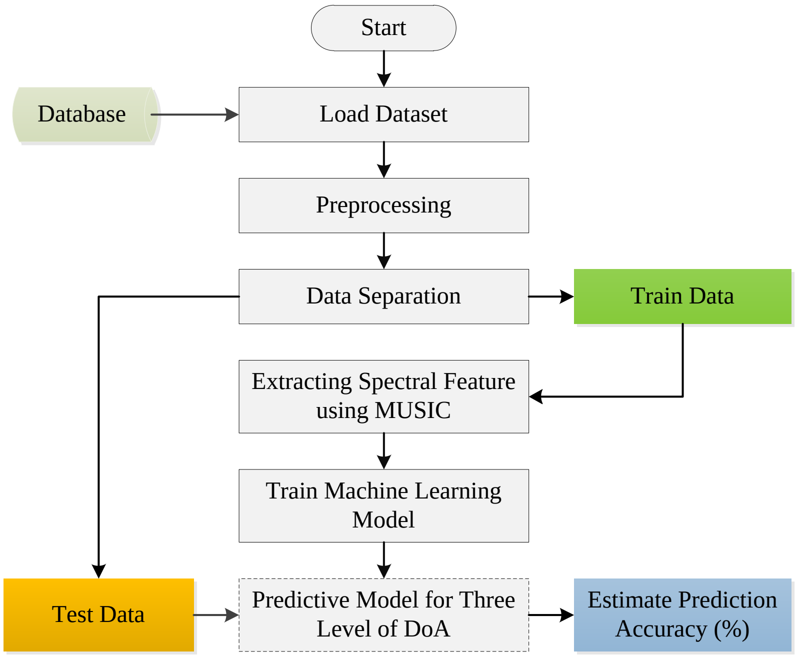


**Figure 3.2:** Methodological steps

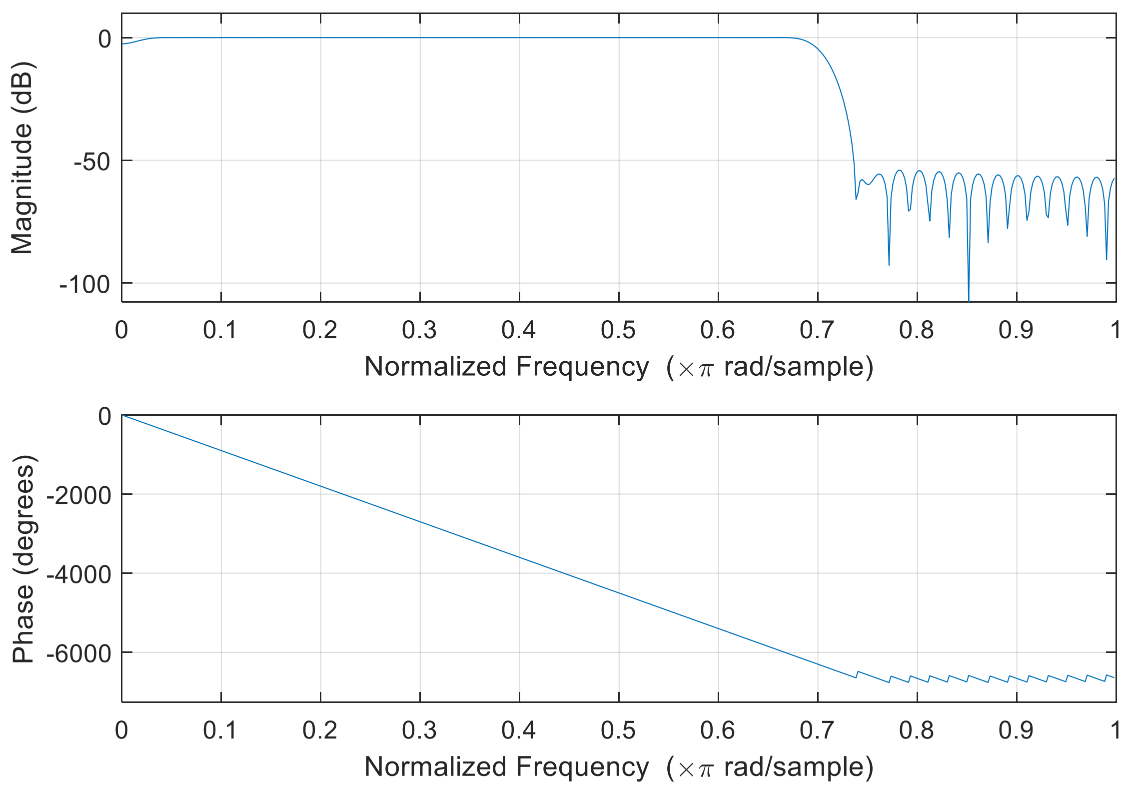


**Figure 3.3:** Magnitude and phase diagram of the applied window-based bandpass FIR filter

### 3.3.2 Data Separation

The dataset used for this work contains the EEG values of the patient during the surgery under anesthetic conditions. In the whole dataset for each case, there are mainly three types of state. The first is **into the deep sleep state (IntoDeep)**, the second is **in the deep sleep state (InDeep)** and the final one is **into the awake-state (InAwake)**. When the patient was given the anesthetic dose from then the recording of the EEG was started. During the whole EEG recording, there are some markers implemented to track the sleep state.

In this dataset, there are some markers to separate the awake state and deep sleep state. For instance, in **Figure 3.4**, the markers are shown by arrows. These marking areas depict no recording of EEG data. Therefore, the data values are almost equal to zero. The first marker or blank area specifies that the patient underway into the deep sleep condition. The data since the first data sample to the first marker can be parted into deep sleep state (**IntoDeep**).

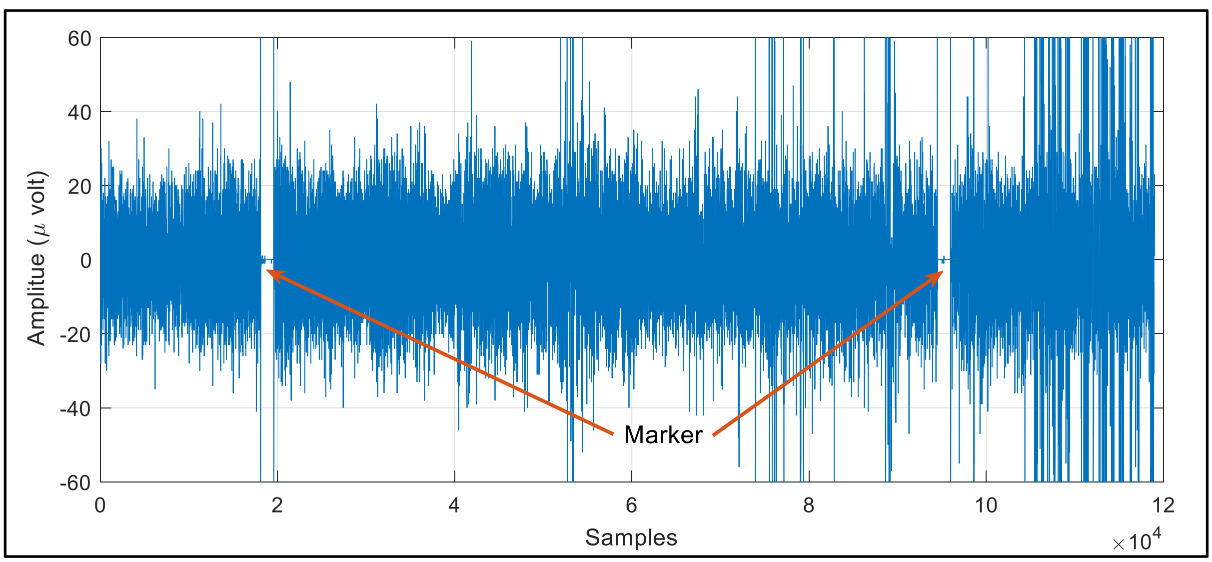


**Figure 3.4:** EEG data with markers

The last marker of the dataset indicates to move of the recovery state from the deep sleep state by the patient which is termed here **InAwake** state. As a result, EEG data of deep sleep state (**InDeep**) can be separated from the very first marker to the starting of the very last marker. Eventually, three different types of states are separated from each patient's EEG signal.

To make the data separation process more understandable, randomly two patients data are selected, they are patient no 13 and 21. According to the markers, the data samples are divided into three separate classes those are presented in **TABLE 3.1**. Also the duration covered by the samples are calculated as,

$$time\,duration(in\,sec) = \frac{Total\,Data\,Samples}{Sampling\,Rate} \tag{3.1}$$

Here, the data sampling rate is 128Hz. Since the patient's age, weight, BMI etc. are different; they are medicated with different doses as well. Therefore, the time required getting into the deep sleep state and recovery times are different. Plus, the surgery types are also different and that's so why the duration of surgery is also different for the different patients that can be perceivable from the information of **TABLE 3.1**. Every 2s data (2×128=256 samples) is considered for single observation.

**TABLE 3.1**: Data samples and observation samples in different state of mind

| **Case No** | **Into Deep** | **In Deep** | **Into Awake** |
|---|---|---|---|
| 13 | 1: 140066<br>( 1094 sec ) | 140067: 444437<br>(2376 sec) | 444438:523540<br>(618 sec) |
| 21 | 1:105607<br>(825 sec) | 105608:1021571<br>(7156 sec) | 1021572:1197760<br>(1376 sec) |

### 3.3.3 Extracting Spectral Feature using MUSIC

MUSIC of multiple class signal classification method is a parametric power spectral density estimation technique. MUSIC method consider that in the presence of Gaussian white noise, ***n***, a signal vector $\boldsymbol{x}$ can be presented as a linear model,

$$\boldsymbol{x} = \boldsymbol{As} + \boldsymbol{n} \tag{3.2}$$

This signal, ***x*** in (3.2) consists of ***p*** complex exponentials of unknown frequency, $\omega$. Here $\boldsymbol{A}$ is a Vandermonde matrix of $M \times p$ dimensions. In this assumption, s is the amplitude vector. The detail definition of ***A***, ***a***, and ***s*** are given in (3.3), (3.4), and (3.5), respectively.

$$\boldsymbol{A} = [\boldsymbol{a}(\omega_1), \boldsymbol{a}(\omega_2), ..., \boldsymbol{a}(\omega_p)] \tag{3.3}$$

$$\boldsymbol{a}(\omega) = [1, e^{i\omega}, e^{i2\omega}, ..., e^{j(M-1)\omega}]^T \tag{3.4}$$

$$\boldsymbol{s} = [s_1, s_2, ..., s_p]^T \tag{3.5}$$

A critical postulation is that number of sources, ***p***, is less than the number of elements in the measurement vector, ***M***, *i.e.*, $\boldsymbol{p} < \mathbf{M}$.

The autocorrelation matrix of ***x*** is the dimension ***M***×***M*** and it can be equated as

$$\boldsymbol{R_x} = AR_s A^H + \sigma^2 I \tag{3.6}$$

where $\sigma^2$ is the variance of noise. Identity matrix is ***I*** of ***M***×***M*** dimension, and $\boldsymbol{R_s}$ is the autocorrelation matrix of ***s*** of order *p*×*p*. The autocorrelation matrix $\boldsymbol{R_s}$ is traditionally estimated using sample correlation matrix

$$\hat{\boldsymbol{R}}_{\boldsymbol{x}} = \frac{1}{n} AXX^{H} \tag{3.7}$$

where $\boldsymbol{N}$ is less than $\boldsymbol{M}$ which is the vector observations number and $\boldsymbol{X} = [x_1, x_2, ..., x_N]$. When it is given the estimation of $\boldsymbol{R_x}$, MUSIC can estimate the signal's frequency content or determine the autocorrelation matrix based on the eigenspace method.

Being $\boldsymbol{R_x}$ a Hermitian matrix, its all eigenvectors $M$=$[v_1, v_2, ..., v_M]$ are orthogonal to each other. Now, if the roots of the characteristic equations i.e., $\boldsymbol{R_x}$'s eigenvalues are arranged in decreasing order, the corresponding eigenvectors $[v_1, v_2, ..., v_p]$ to the $p$ largest eigenvalues span the signal subspace $U_S$. The remaining corresponding eigenvectors ($M$-$p$) equal to $\sigma^2$ and distance the noise subspace $U_N$, which is also orthogonal to the signal subspace, $U_S \perp U_N$.

It can be noted that for $M$=$p$+1, MUSIC is similar to Pisarenko harmonic decomposition. The overall concept of MUSIC method is to utilize all eigenvectors that span the noise subspace to progress the enactment of the Pisarenko estimator. Since any signal vector $e$ that exist in in the signal subspace $e \in U_S$ must be orthogonal to the noise subspace, $e \perp U_N$, it must be that $e \perp v_i$ for all eigenvectors $\{v_i\}_{i=p+1}^{M}$ that spans the noise subspace. To measure the degree of orthogonality of $\boldsymbol{e}$ with respect to all the $v_i \in U_N$, the MUSIC algorithm describes a squared norm as

$$d^2 = \left\|U_N^H e\right\|^2 = e^H U_N U_N^H e = \sum_{i=p+1}^{M} \left|e^H v_i\right|^2 \tag{3.8}$$

where the matrix $U_N = [v_{p+1},..., v_M]$ is the matrix of eigenvectors that span the noise subspace $U_N$. If $e_i \in U_S$, then $\boldsymbol{d}^2 = 0$ as implied by the orthogonality condition. Taking a reciprocal of the squared norm expression generates high-pitched peaks at the dominant signal frequencies. The estimation function for frequency spectra obeying the MUSIC (or the pseudo-spectrum) can be calculated as,

$$\hat{P}_{MU}(e^{jw}) = \frac{1}{e^H U_N U_N^H e} = \frac{1}{\sum_{i=p+1}^{M} \left| e^H v_i \right|^2} \tag{3.9}$$

where $v_i$ denotes the noise eigenvectors and $e = [1\, e^{j\omega}\; e^{j2\omega} \ldots\; e^{\,j(M\text{-}1)\omega}]^T$ presents the entrant steering vector. The positions of the $p$ highest peaks of the estimating function contribute the frequency spectra.

MUSIC overtakes simple approaches such as harvesting peaks of DFT (Discrete Fourier Transform) spectra even in noise space, when the component number is identified earlier, because it feats information of this number to disregard the noise in its concluding results. Unlike DFT, it is capable to guess frequencies with higher accuracy. This is because its estimation function can be assessed for any frequency, not just those of DFT bins. Therefore, MUSIC offers a super-resolution form.

Its main shortcoming is it's requirement of the number of components to be acknowledged priory, so the original technique is used in particular cases. Methods those are related to estimate the source component number that purely comes from statistical properties of the autocorrelation matrix (Fishler, 2005).

In this project, the spectral information that founds from the MUSIC algorithm i.e., estimated power spectral density from single channel EEG data was considered as features of that signal. As previously discussed single channel EEG data of each patient is divided into three different classes. Before developing the predictive model from this data classes feature extraction is needed to transform the data into a new domain and specify the data in more distinctive approach so that the machine learning process can easily understand the data differentiability and can make a correct predictive model. In this work, MUSIC algorithm was used to transform the data into the signal's power spectral density. This power spectral density pattern can be set within a predefined number (at least greater than the two times of its sampling frequency). In this case, the number was selected 512 as the sampling rate is 128, fairly greater enough than the theoretical convention.

A sample EEG signal and its extracted feature power spectral information are given in **Figure 3.5**. Here the order was selected 5 and the length of FFT (Fast Fourier Transform) was considered 512. Eventually the PSD bin has been found 257, just 50% of the length as the other 50% of PSD is the mirror of the current view. In the **Figure 3.5**, there are two different PSD estimation result, although they provide same results. The first one is in watt per Hertz unit and the second one is presented as its dB values. In general practice, PSD is presented with its dB values. This PSD value of each trial of different DoA is considered as the feature of each trial signal.

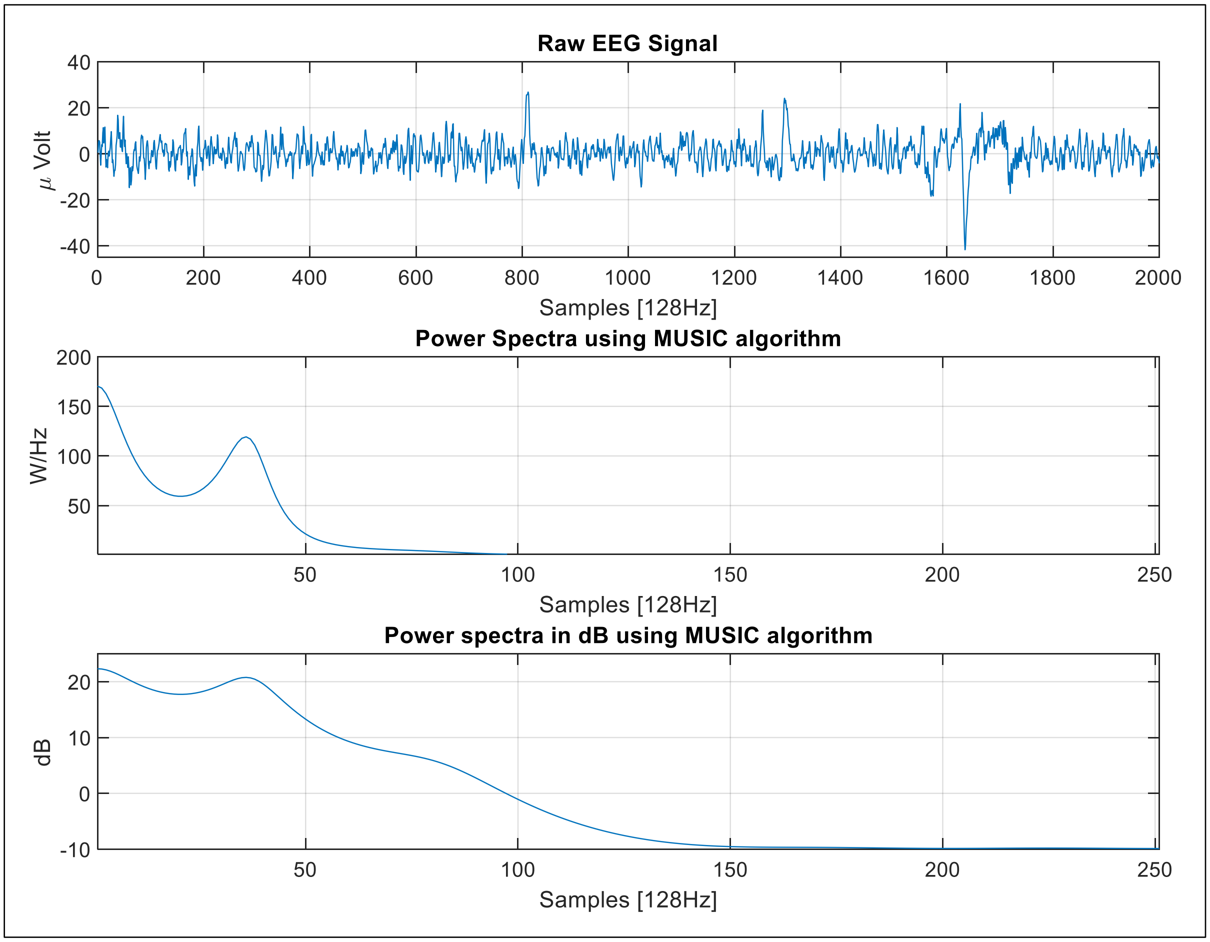


**Figure 3.5:** PSD estimation by MUSIC algorithm from a randomly selected EEG data

### 3.3.4 DoA Prediction

According to the proposed model, the EEG signals are separated into three different categories. Therefore, these three categories will be considered as the classes of machine learning based classification or prediction problem. The EEG signals of three categories will be subdivided into 2 second window signals and eventually they will be considered as the trials of each class. According to the length of the signals of different classes the number of trials will be different. Then each trial will go under MUSIC algorithm of specific order for feature extraction. Then, the extracted features will be used for feeding the machine learning process. A certain amount of trials, say 50%, will be used for training purpose and rest 50% will be used for testing or predicting the learning level of the machine. Therefore, in this state the objective of this method is to choose a classifier, select a suitable learning algorithm, validate the process, and test the efficiency of the classifiers. In this subsection, this process is described gradually.

#### 3.3.4.1 Classifier

For classification, the ANN (artificial neural network) was used as a supervised learning model. As in this work we are dealing with three class EEG data, the features of the targeted classes are arranged according to the input styles of the ANN model.

ANN is a popular technique to apply machine learning to data by examining it via a network of layers that make choices (Goel, 2022). The technique's name comes from the fact that the algorithm's structure resembles that of a human brain. Although these artificial neural networks are not identical to the brain's decision-making process, they do have certain commonalities. Neurons in the brain, for example, are connected and contain dendrites that accept inputs. It generates an electric signal in its axon and transmits it to other neurons through axon terminals. Artificial neural networks, meanwhile, are made up of decision functions, or nodes, that are connected by axon-like edges. Different sorts of nodes are used to make up the layers of a neural network. Initially, they are generally rather broad. The first layer is made up of nodes that are made up of raw input data (such as numbers, text, picture pixels, or sound). Each input node delivers information to the next tier of nodes through edges in the network, allowing information to reach them (Beibei, 2022). Each network edge has a numerical weight that may be adjusted depending on your performance. This is known as the '**activation function**', and it specifies how many linked edges must achieve a specific threshold before a neuron may be started at a lower layer. It will not operate if the total of all linked edges does not match the defined threshold. As a consequence, it's either all or nothing. Furthermore, each edge's weights are distinct, implying that the nodes fire at various times, preventing them from yielding the same solution.

In supervised learning, the model's predictions are compared against the known-to-be-correct actual output (Shurrab, 2022). The difference between these two outcomes is referred to as the "cost," and the value of that difference is referred to as the "value of the cost." The purpose of training is to reduce the cost value until the model's prediction is extremely near to the actual result. This is accomplished by gradually adjusting the network's weights until the lowest potential cost value is discovered. The neural network is being trained during this time. It's known as back-propagation. Back propagation does not go from left to right when data is supplied into a network; rather, it does backward propagation.

For an ANN to learn and grasp anything sophisticated, the Activation function is essential. Their main job is to turn an ANN node's input signal into an output signal. The following rung of the stack receives this output signal. The output signal is essentially a linear function if no activation function is employed (one-degree polynomial). Although a linear function is easy to solve, its complexity and power are limited.

Without the activation function, no model can learn and model complex data such as images, movies, audio, voice, and so on. A general conception of an activation function and its operation is given in **Figure 3.6**.

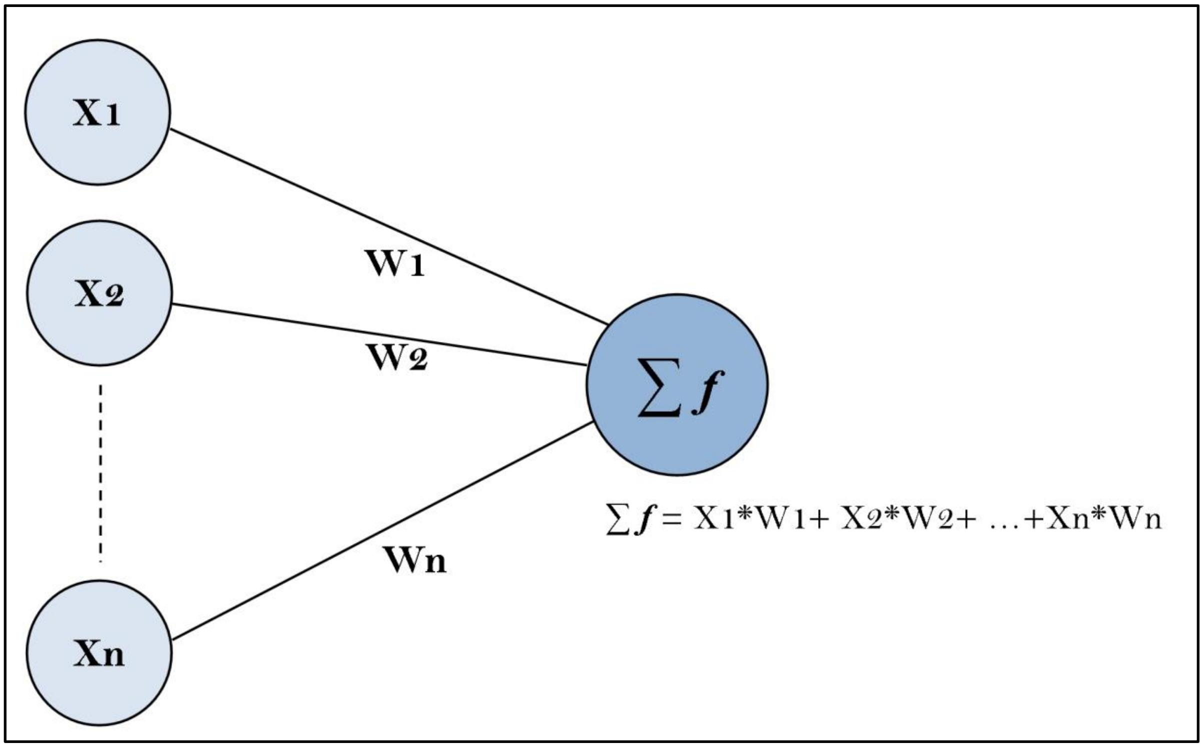


**Figure 3.6:** Gross conception about the activation function of neural network

### 3.3.4.2 Building a Neural Network

There are input layers, hidden layers, and output layers in a typical neural network as shown in **Figure 3.7**. The data is initially delivered to the input layer, where it is analyzed for characteristics. The input characteristics are then examined and processed by the hidden layer(s), and the final result is shown on the result layer. Because, like human eyesight, the intermediary layers process items between the input and output levels without being observed, they are said to be concealed.

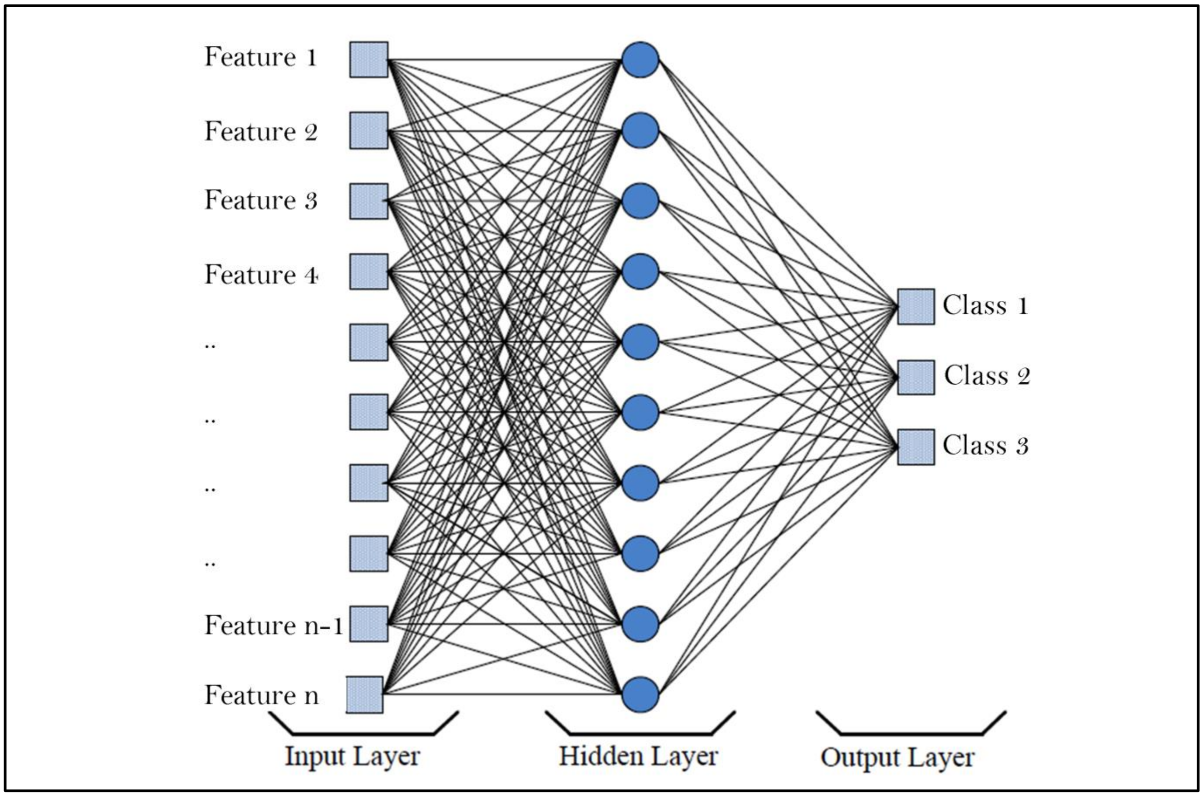


**Figure 3.7:** The main building blocks of a neural network

We immediately conceive of it as a square when we see four lines joined in a square pattern. We're not aware of how much mental effort it takes to visualize the four polylines (input) as a square (output). In the same manner, neural network functions. They divide data into layers and analyze the non-visible levels to get at a final output.

As more hidden layers are added to the network, the model's ability to look at complex patterns also gets better. This is why models with a lot of layers are called "deep learning" to show how well they can process things. When you build a neural network, there are many ways to put the nodes together. The simplest way is to use a feed-forward network, which means that signals only move in one direction and there is no loop in the network. There are many different types of feed-forward neural networks, but the perceptron is the simplest.

#### 3.3.4.3 Training and Validation Process

For the training a supervised classifier especially an artificial neural network, there are several available learning algorithms like: *i*) Gradient descent (Xue, 2022), *ii*) Newton method (Bertsekas, 2022), *iii*) Conjugate gradient (Kim, 2023), *iv*) Quasi-Newton method (Likas, 2000), *v*) Levenberg-Marquardt algorithm (Nguyen, 2021), etc. In this project, for training our ANN based model Levenberg-Marquardt (LM) algorithm is used. A brief understanding about LM algorithm is presented here.

The LM algorithm is premeditated to function particularly with the loss functions that take the sum of the squared form of the error. It works devoid of calculating the precise Hessian matrix. In its place, it works through the gradient vector and the Jacobian matrix. Contemplate a loss function that forms a sum of squared errors,

$$f = \sum_{i=1}^{m} error_i^2 \tag{3.10}$$

Here $m$ is the training samples number. Jacobian matrix of the loss function can be defined as the containing derivatives of the errors considering the parameters as,

$$J_{i,j} = \frac{\partial}{\partial w_j}(error_i) \tag{3.11}$$

for $i$=1, ...,$m$ and $j$=1,...,$n$. Where $m$ is the number of samples in the data set, and $n$ is the number of parameters in the ANN. It should be noted that, Jacobian matrix size is $m \times n$. We can compute the gradient vector of the loss function as,

$$\nabla f = 2J^T.\bar{e} \tag{3.12}$$

Here, $\bar{e}$ represent all error vectors. Lastly, Hessian matrix can be approximated by the following expression.

$$Hf \approx 2J^T.J + \lambda I \tag{3.13}$$

Where $\lambda$ is for damping factor and it assures the positivity of the Hessian and identity matrix is $I$. The parameters improvement process is presented here in (3.14) along with the expression of the LM algorithm,

$$w^{(i+1)} = w^{(i)} - (J^{(i)T}.J^{(i)} + \lambda^{(i)} I)^{-1}.(2J^{(i)T}.e^{(i)}) \tag{3.14}$$

for $i$=0,1,...

If the damping parameter ($\lambda$) can be considered zero, it present pure Newton's method. Instead, when damping parameter is large, with a small training rate it becomes gradient descent.

The damping parameter is adjusted to be large so that the first apprises are trivial steps in the direction of gradient descent.

The **Figure 3.8** represents a training process of a neural network with a state diagram for the the LM algorithm. Here, first step calculates the loss, then the gradient, and finally the Hessian approximation. Then, the $\lambda$ is attuned to decrease the loss at each iteration.

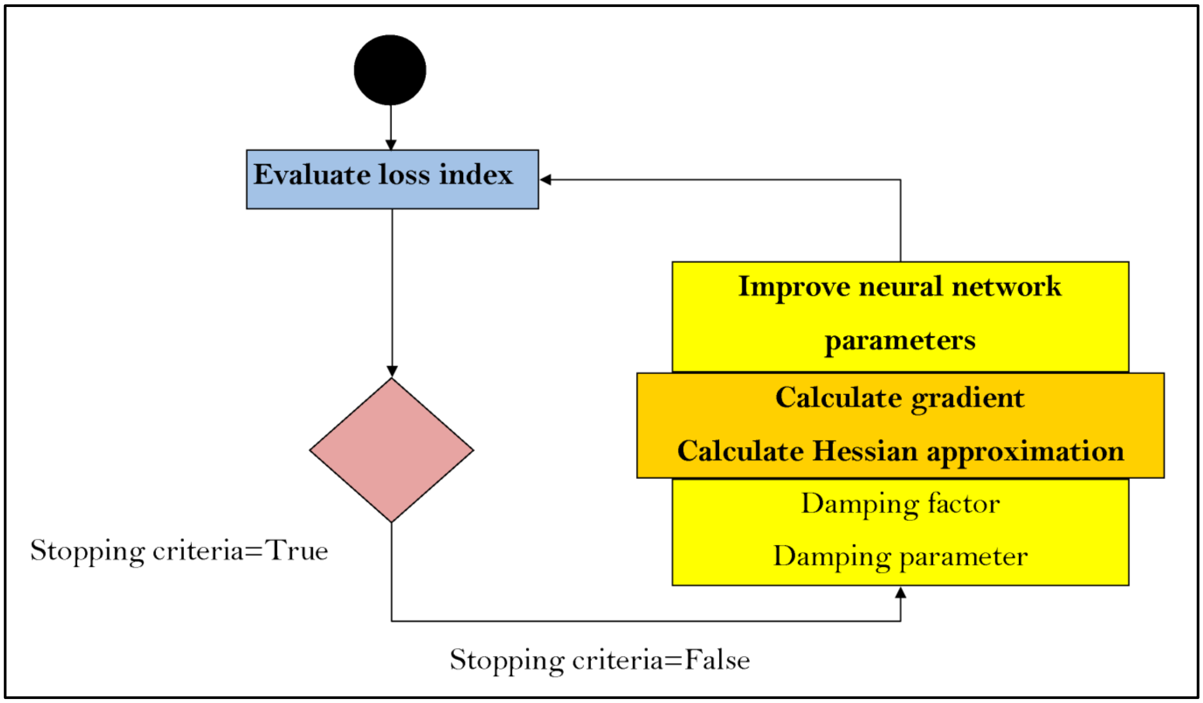


**Figure 3.8:** State diagram for the training process by the LM algorithm

As it is observed that the methodology of LM algorithm tailored for functions of the type sum-of-squared-error, it marks to be very speedy when the training process of ANN measuring its errors.

However, this method contains some problems:

(*i*) It cannot minimize functions such as the root mean squared error or the cross-entropy error.

(*ii*) The Jacobian matrix becomes enormous for big data sets and neural networks, requiring much memory.

Therefore, the LM algorithm is not suitable for big dataset. Since this work has small dataset, this algorithm works well in learning the network.

#### 3.3.4.4 Prediction

The determination of testing is to relate the results from the ANN against targets in a self-regulating dataset. If the testing metrics are measured ok, the ANN can transport itself to the so-called deployment phase. The authentication methods depend on the following application types: *i*) Approximation testing methods, *ii*) Classification testing methods, and *iii*) Forecasting testing methods.

The most common testing methods in the field of classification problems is Confusion matrix In the confusion matrix, the rows represent the target classes in the data set and the columns represent the corresponding output. The diagonal cells in the confusion table describe the correctly classified cases, and the off-diagonal cells describe the number of the misclassified cases. Note that the output from the neural network is a probability in general. Therefore, the decision threshold predicts the class information. A confusion matrix from a prediction result of three class testing set is shown in **Figure 3.9**.

## 3.4 Conclusions

The methodological steps described here are applied on the dataset and the results found for these steps are presented in the next section with necessary discussions.

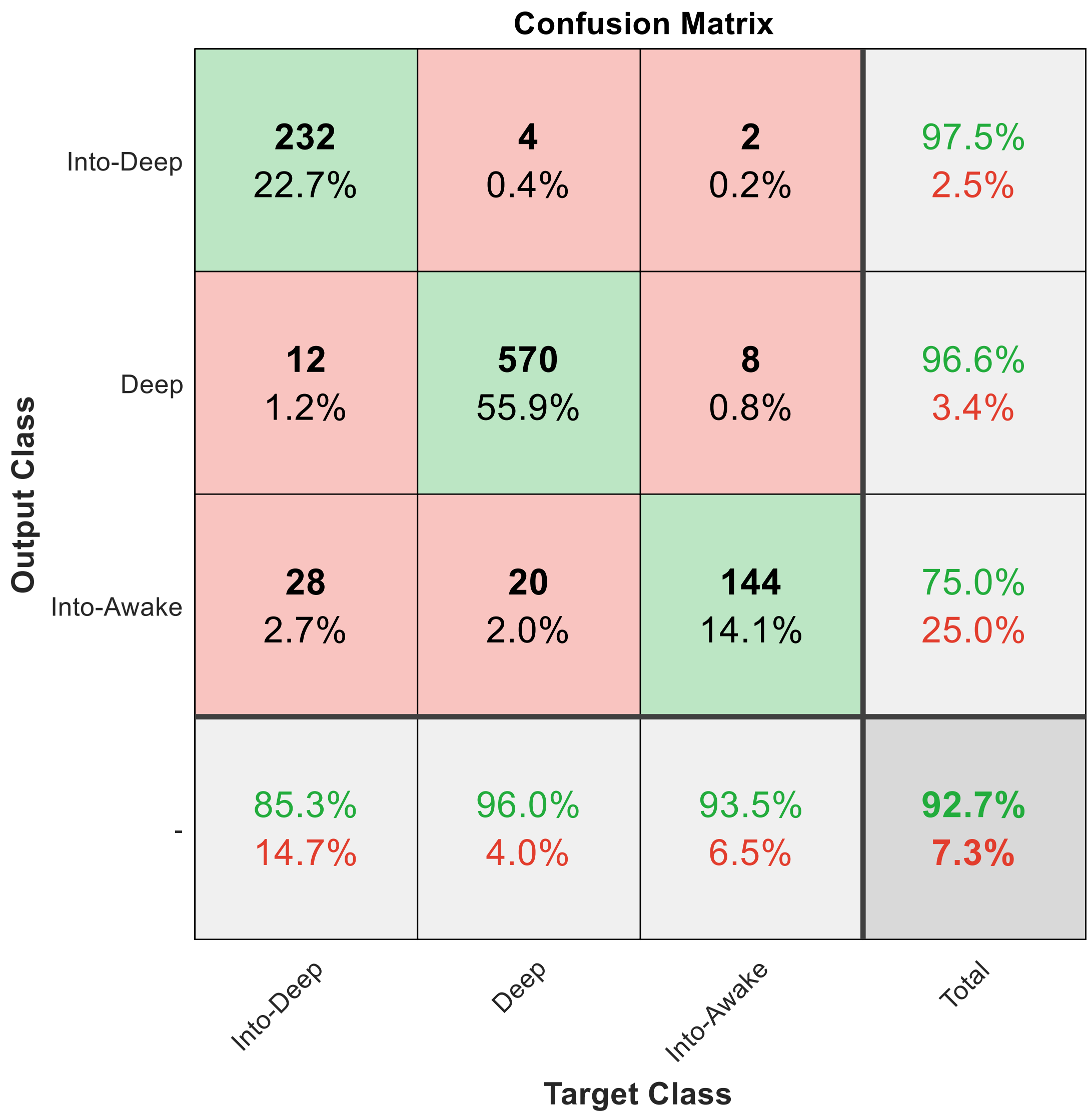


**Figure 3.9:** Confusion matrix of the prediction result of three class testing dataset

# CHAPTER 4

# RESULTS AND DISCUSSIONS

## 4.1 Preprocessing

The first preprocessing step applied on the dataset was filtering. All data are filtered with a band-pass filter considering the band is 0.3-45Hz. This band-pass filter was designed using an FIR (Finite Impulse Response) filter with hamming window of 100 orders. The resulting filtered data has been shown in **Figure 4.1** with the corresponding raw EEG data so that the filtering effect can be visible. This filtering effect removes the unnecessary spikes and noises from the EEG data. Since the filter takes the frequency content up to 45 Hz, the power line noise (50Hz/60Hz) get removed from the raw EEG signal.

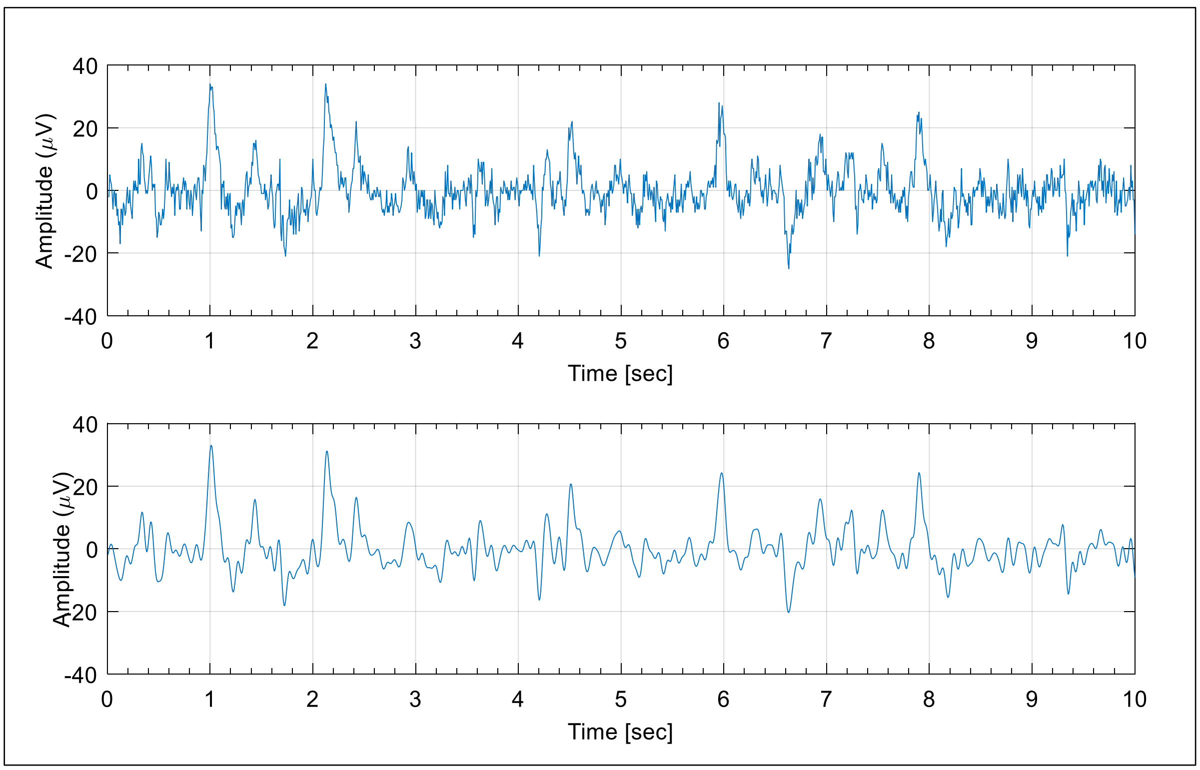


**Figure 4.1:** Raw and filtered EEG signal

There is a direct impact of filtering on the feature extraction process. To make it understandable a comparative analysis of spectral information is given in **Figure 4.2**. In this figure, two types spectral information are extracted using MUSIC algorithm. The variations in the spectra are more accurate and visible for the filtered data whereas almost no variation is found in the raw EEG data. The change in the spectra is the key concern of different class data. It clarifies the effect of filtering.

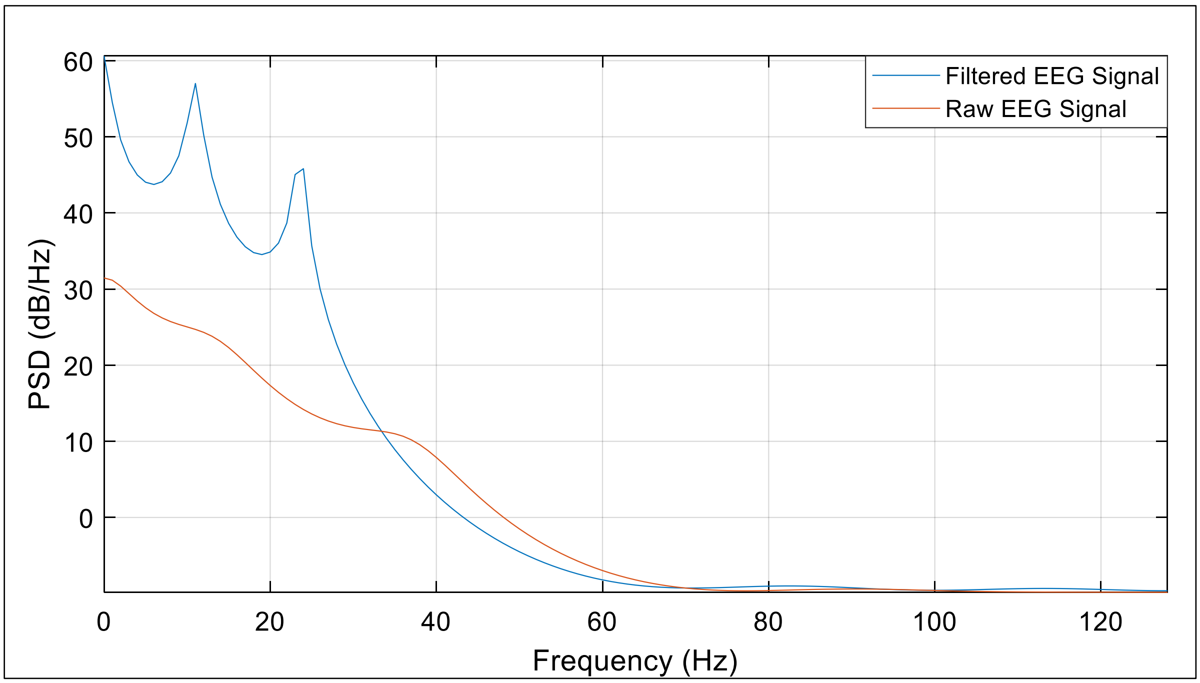


**Figure 4.2:** Extracted spectra of raw and filtered EEG signal using MUSIC algorithm

### 4.2 Data Separation

It has been already discussed in the methodology section that each participants' data is divided into three categories those are *i*) IntoDeep, *ii*) InDeep and (*iii*) InAwake**.** This data separation process creates our three-class classification problem. Here, three categories are three classes for modeling the machine learning predictor for sleep state detection. There are 24 patients in the dataset. Therefore, 24 different set of three classes were divided.

In **Table 4.1**, the information is structurally tabulated. The table presents the samples and seconds are in three different sleep states during subject-wise operations. The time duration in sec is calculated from the dividing the samples span by the signal's sampling rate. It is already mentioned that the sampling rate was 128Hz.

**Table 4.1**: Data samples and observation samples in different state of mind

| Case No | IntoDeep | | InDeep | | IntoAwake | |
|---|---|---|---|---|---|---|
| | *Samples* | *Second* | *Samples* | *Second* | *Samples* | *Second* |
| 1 | 1:68136 | 532 | 68137:412328 | 2689 | 412329:481384 | 539 |
| 2 | 1:65092 | 508 | 65093:600366 | 4182 | 600367:625664 | 198 |
| 3 | 1:13570 | 106 | 13571:1619012 | 12543 | 1619013:1673152 | 423 |
| 4 | 1:66606 | 520 | 66607:448826 | 2986 | 448827:499040 | 392 |
| 5 | 1: 66944 | 523 | 66945:296117 | 1790 | 296118:309728 | 106 |
| 6 | 1:64782 | 506 | 64783:598646 | 4171 | 598647:643392 | 350 |
| 7 | 1: 67484 | 527 | 67485:755689 | 5377 | 755690:775008 | 151 |
| 8 | 1:32030 | 250 | 32031:949516 | 7168 | 949517:1017568 | 532 |
| 9 | 1:62016 | 484 | 62017: 749987 | 5375 | 749988:765172 | 119 |
| 10 | 1:34947 | 273 | 34948:723150 | 5377 | 723151:793568 | 550 |
| 11 | 1:64270 | 502 | 64271:1667850 | 12528 | 1667851:1716992 | 384 |
| 12 | 1:63852 | 498 | 63853:2581771 | 19671 | 2581772:2603296 | 168 |
| 13 | 1:62155 | 485 | 62156:444429 | 2987 | 444430:523540 | 618 |
| 14 | 1:60974 | 476 | 60975:366266 | 2385 | 366267:399029 | 256 |
| 15 | 1:138990 | 1085 | 138991:1591343 | 11347 | 1591344:1687072 | 748 |
| 16 | 1:49880 | 389 | 49881:891008 | 6571 | 891009:917760 | 209 |
| 17 | 1:62836 | 490 | 62837:903952 | 6571 | 903953: 972640 | 537 |
| 18 | 1:63642 | 497 | 63643:445853 | 2986 | 445854:474336 | 223 |
| 19 | 1:64793 | 506 | 64794:523615 | 3585 | 523616:557440 | 264 |
| 20 | 1:59379 | 463 | 59380:1205994 | 8958 | 1205995:1247956 | 328 |
| 21 | 1:27890 | 217 | 27891:1174696 | 8959 | 1174697:1197760 | 180 |
| 22 | 1:57186 | 446 | 57187:286514 | 1792 | 286515:296192 | 76 |
| 23 | 1:109227 | 853 | 109228:717726 | 4754 | 717727:745184 | 215 |
| 24 | 1:66726 | 521 | 66727:448902 | 2986 | 448903:483648 | 271 |

Every 5 sec data or 5×128=640 samples of each sleep state is considered as one trial for that sleep-state or that class. There are three classes of data in this problem. Since the patients are different in age, sex, disease, etc., their duration of surgery was also different. Therefore, the trials of three classes are not equal for a patient, whether the conditions of every patient are also dissimilar.

### 4.3 Feature Extraction

After filtering and separating the class-wise trials, the feature extraction step is considered for processing. Before, feature extraction by MUSIC method, according to the proposed method it is necessary to set the optimal order of MUSIC model for the signal. In this regard, three different order MUSIC model was tested in working signal on both filtered and raw EEG signal. These results are given in **Figure 4.3**, **Figure 4.4**, and **Figure 4.5**, respectively. From the results, it is noticeable that the maximum variation has been found in order 7. Furthermore, in order 7 the spectrum achieves three peaks which are least necessary for classifying three different classes. If the order is increased, the variation between the raw and filtered signal will also be increased along with the number of peaks. Since increasing the order value increases the computational load, we cannot go further the order 7, and also we cannot lower the order size because an order less than 7 cannot give us three peaks. In this logic, order 7 for MUSIC spectrum estimation is optimal.

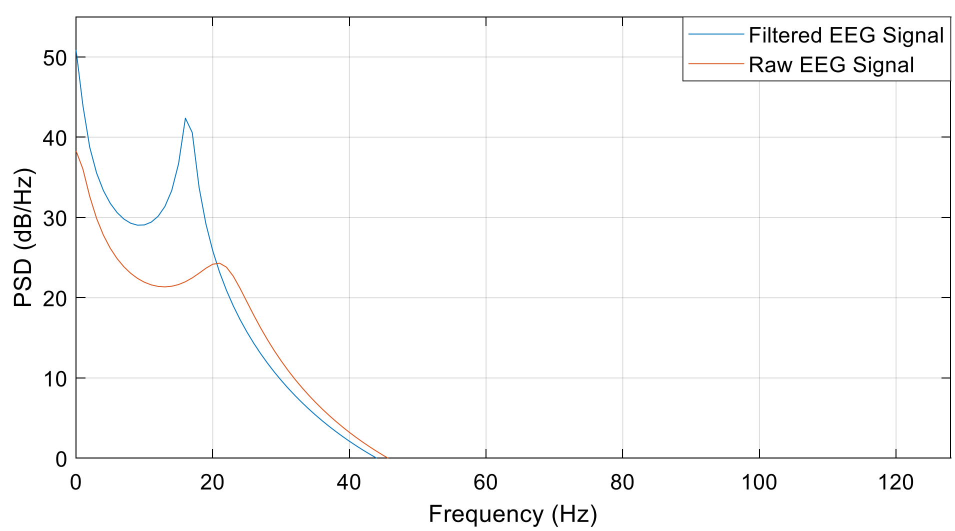


**Figure 4.3:** Comparison between MUSIC spectrum of raw and filtered EEG signals considering the order of MUSIC is 3

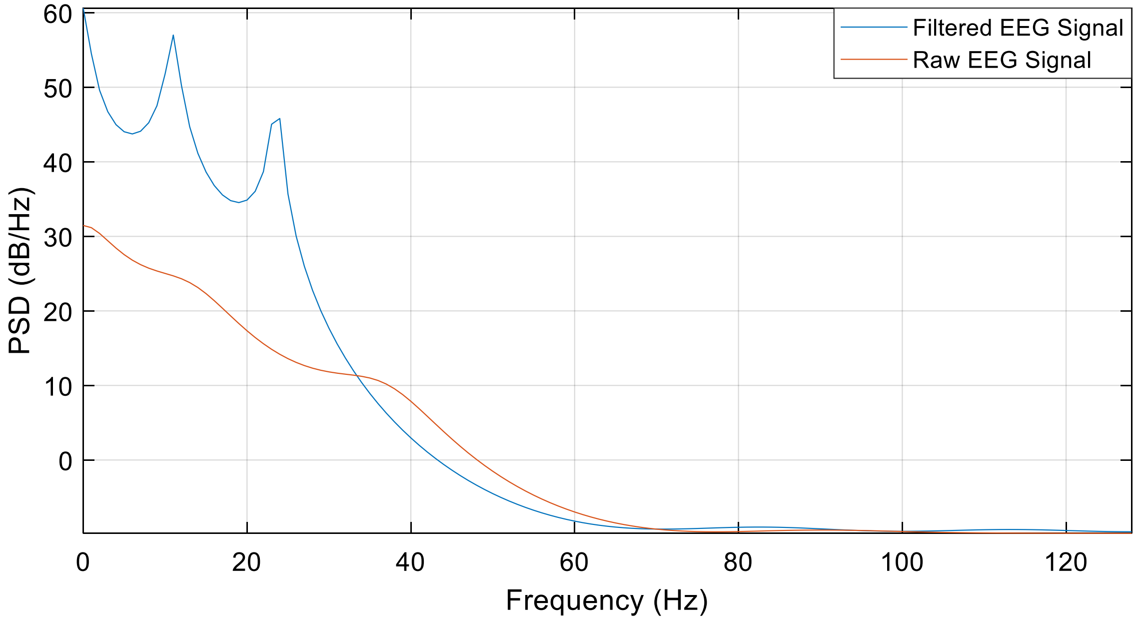


**Figure 4.4:** Comparison between MUSIC spectrum of raw and filtered EEG signals considering the order of MUSIC is 5

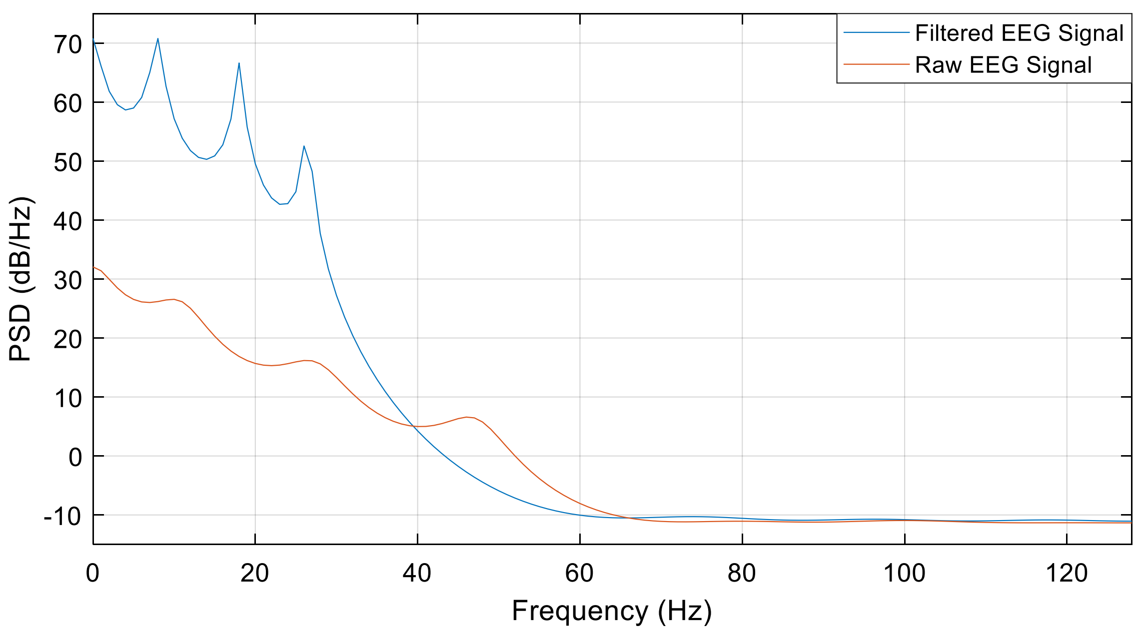


**Figure 4.5:** Comparison between MUSIC spectrum of raw and filtered EEG signals considering the order of MUSIC is 7

Since the MUSIC spectrum of order 7 show maximum variation in the spectra concerning the raw signal, this order is considered to extract feature from the signal trials.

A sample signal of subject 2 was taken of three different sleep states and their MUSIC spectra are estimated and shown in **Figure 4.6**. In this figure, the changes in the pattern of three different sleep states are clearly perceivable. The idea behind the feature extraction process came from these kinds of variations found in the pattern of the MUSIC spectra of different classes. Eventually, considering order 7, the MUSIC model is used to extract the spectra and the values of the spectra are considered as the feature of that signal class.

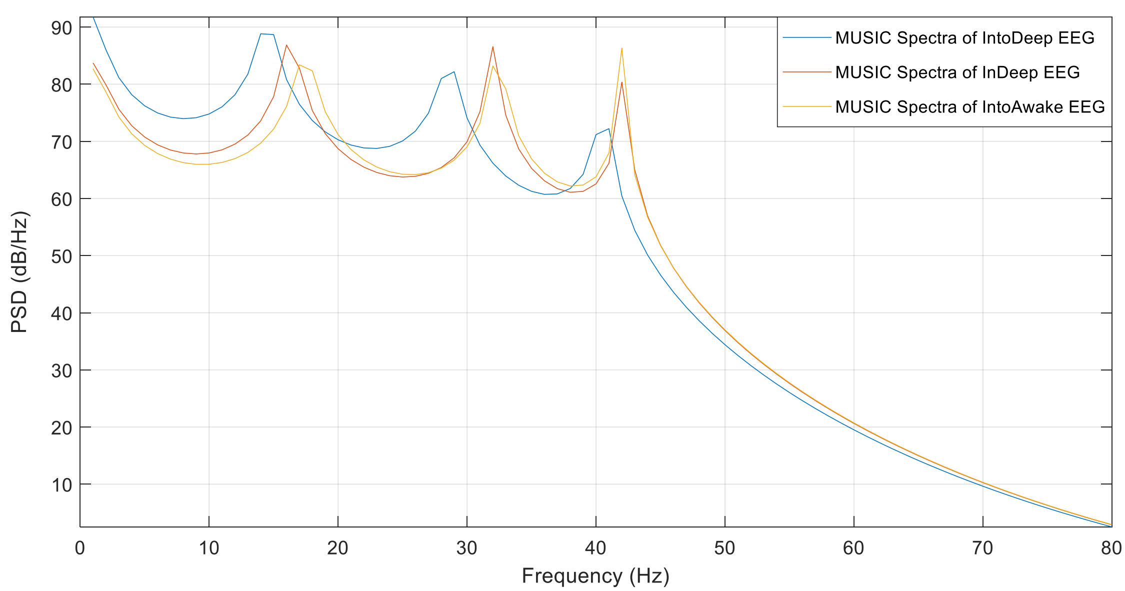


**Figure 4.6:** Comparison between different states' MUSIC spectra considering the order of MUSIC is 7. (*Here, the EEG data of Patient 2 is used*)

## 4.4 Subject-Dependent Classification

These features are fed to the neural network as discussed in the methodology section and a predictive model was developed. Using that predictive model the testing data are classified. For example on the results of different subjects, the predictive accuracy (testing class accuracy) of the DoA is preserved. The training and testing ratio was considered 50:50. Since the data samples are different in the different cases. Therefore the total samples for each class for each case are tabulated as the estimated trials for training and testing. Here, the trials are taken for every 2 sec of data. This result is presented in **Table 4.2**. Since the duration of three different sleep states is different, the number of trials per class is not equal. Therefore, all trials of each class for every patient are tabulated in **Table 4.2**.

The best way to show the classification or prediction accuracy is by confusion matrix. The classification results of the first 5 patients are presented by a confusion matrix. They are given in **Figure 4.7**, **Figure 4.8**, **Figure 4.9**, **Figure 4.10**, and **Figure 4.11,** respectively. All these results are given in confusion matrix form that helps to understand the detailed scenario of classification in every case and every class. From the results, misclassified trials can also be observed. For instance, in the case of **Figure 4.7**, the total classification accuracy is 85.1% whereas the individual class contribution for the three classes is 84.9%, 85.9%, and 81.5%, respectively. Although the contribution of class 3 is less, the trial number of class 2 leads to the total classification accuracy in this case due to its very high amount of trials.

By similar procedure, classification accuracies of the rest subjects are also estimated. The results are tabulated in **Table 4.3**. From the results, it is found that the average predicting accuracy of the proposed model is **89.07±3.58**.

**Table 4.2:** The possible trials in training and testing the model for all the experimenting patients

| Case No | IntoDeep | | InDeep | | IntoAwake | |
|---|---|---|---|---|---|---|
| | *Train Trials* | *Test Trials* | *Train Trials* | *Test Trials* | *Train Trials* | *Test Trials* |
| 1 | 53 | 53 | 269 | 269 | 54 | 54 |
| 2 | 51 | 51 | 418 | 418 | 20 | 20 |
| 3 | 11 | 11 | 1255 | 1255 | 43 | 43 |
| 4 | 52 | 52 | 299 | 299 | 39 | 39 |
| 5 | 53 | 53 | 179 | 179 | 11 | 11 |
| 6 | 51 | 51 | 417 | 417 | 35 | 35 |
| 7 | 53 | 53 | 538 | 538 | 15 | 15 |
| 8 | 25 | 25 | 717 | 717 | 53 | 53 |
| 9 | 49 | 49 | 538 | 538 | 12 | 12 |
| 10 | 28 | 28 | 538 | 538 | 55 | 55 |
| 11 | 50 | 50 | 1253 | 1253 | 39 | 39 |
| 12 | 50 | 50 | 1967 | 1967 | 17 | 17 |
| 13 | 49 | 49 | 299 | 299 | 62 | 62 |
| 14 | 48 | 48 | 239 | 239 | 26 | 26 |
| 15 | 109 | 109 | 1135 | 1135 | 75 | 75 |
| 16 | 39 | 39 | 657 | 657 | 21 | 21 |
| 17 | 49 | 49 | 657 | 657 | 54 | 54 |
| 18 | 50 | 50 | 299 | 299 | 23 | 23 |
| 19 | 51 | 51 | 359 | 359 | 27 | 27 |
| 20 | 47 | 47 | 896 | 896 | 33 | 33 |
| 21 | 22 | 22 | 896 | 896 | 18 | 18 |
| 22 | 45 | 45 | 179 | 179 | 8 | 8 |
| 23 | 86 | 86 | 476 | 476 | 22 | 22 |
| 24 | 52 | 52 | 299 | 299 | 27 | 27 |

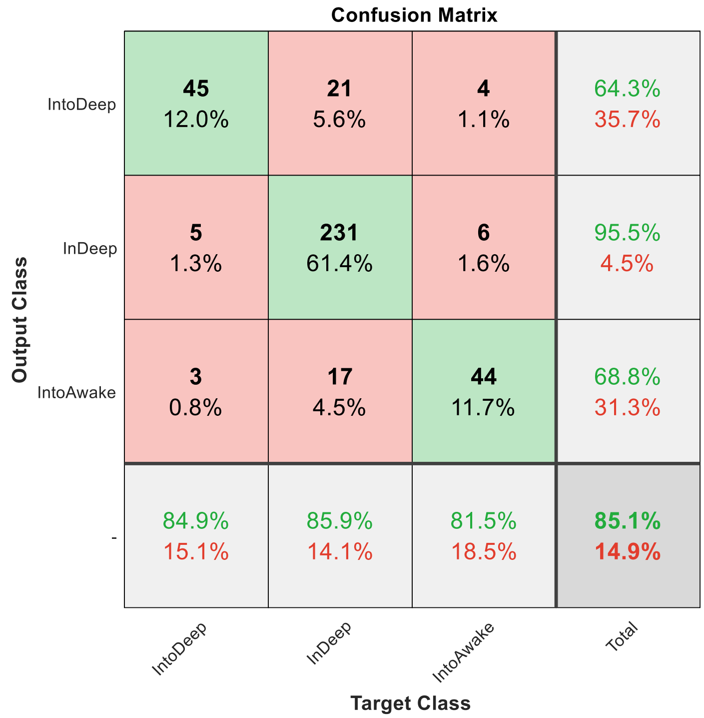


**Figure 4.7:** Classification accuracy of the model with its confusion matrix for the subject 1

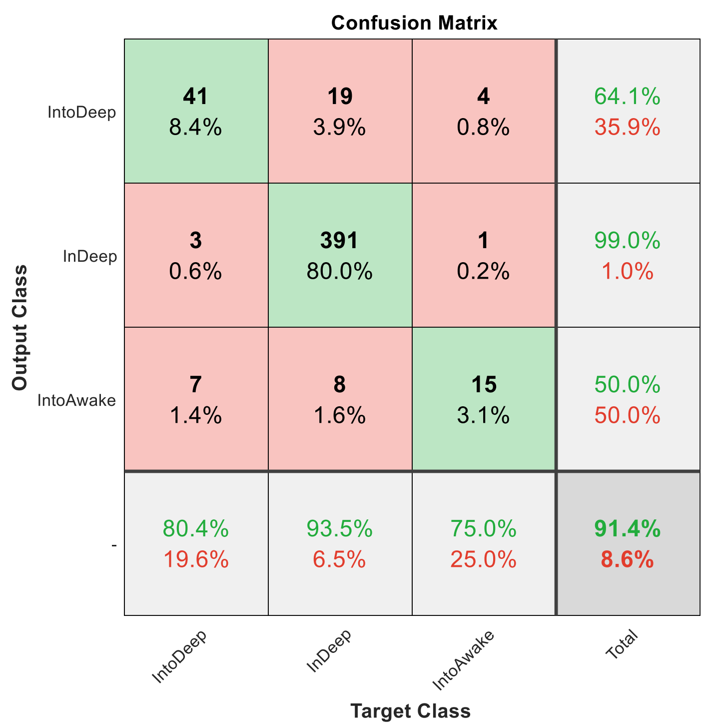


**Figure 4.8:** Classification accuracy of the model with its confusion matrix for the subject 2

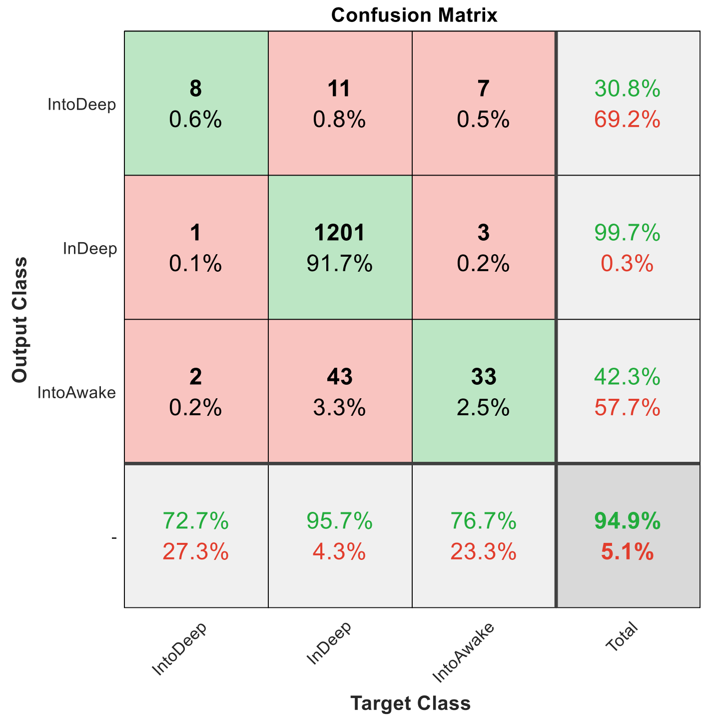


**Figure 4.9:** Classification accuracy of the model with its confusion matrix for the subject 3

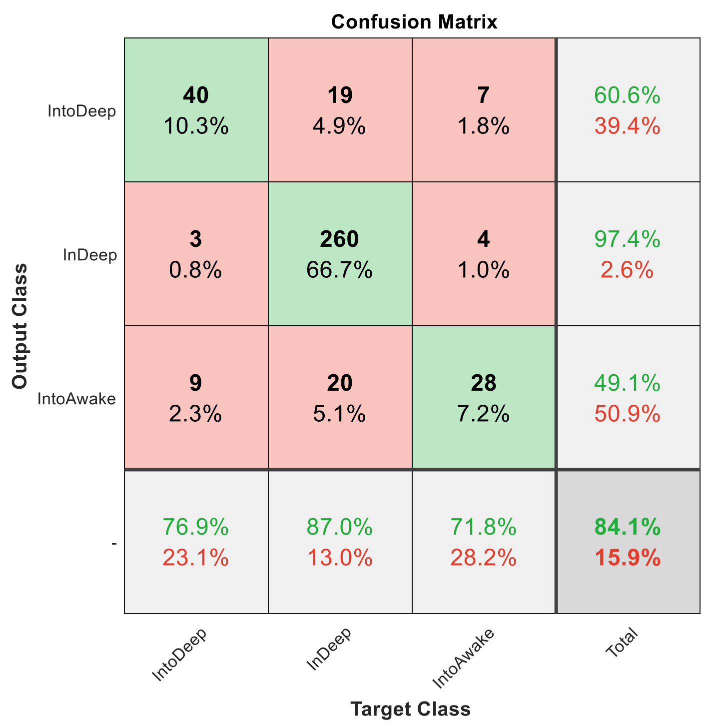


**Figure 4.10:** Classification accuracy of the model with its confusion matrix for the subject 4

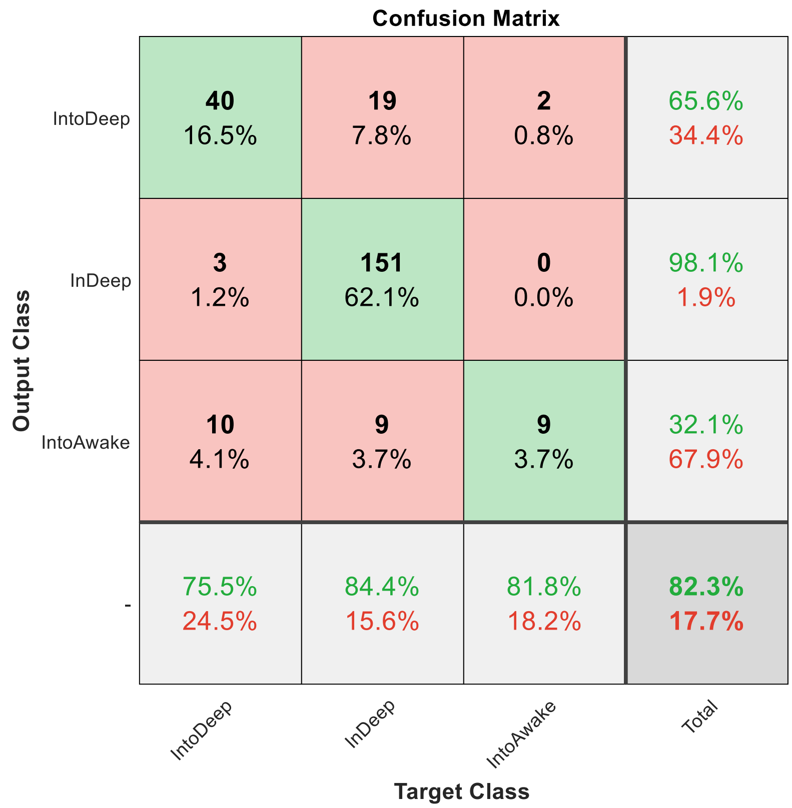


**Figure 4.11:** Classification accuracy of the model with its confusion matrix for the subject 5

One major thing to discuss regarding the previous confusion matrices is that the trial number of three different classes is different. This variation has a significant role in total classification accuracy. The total accuracy will mostly be dependent on the number of accurately classified classes. Since in this problem, the highest duration has been taken by the surgery period, the testing trials of class 2 are higher than that of the other two classes. This factor leads to the total classification accuracy. Detection of the sleep states or deep sleep states is most important during surgery. Therefore, the total accuracy led by class 2 eventually gives us the right conception of the efficacy of the EEG signal to predict the deep sleep state.

**Table 4.3:** Classification accuracy of all subjects

| Subject ID | Classification Accuracy (%) | Subject ID | Classification Accuracy (%) |
|---|---|---|---|
| Patient 1 | 85.1 | Patient 13 | 91.1 |
| Patient 2 | 91.4 | Patient 14 | 89.2 |
| Patient 3 | 94.4 | Patient 15 | 93.4 |
| Patient 4 | 84.1 | Patient 16 | 90.5 |
| Patient 5 | 82.3 | Patient 17 | 92.6 |
| Patient 6 | 88.4 | Patient 18 | 93.8 |
| Patient 7 | 84.9 | Patient 19 | 87 |
| Patient 8 | 91.1 | Patient 20 | 82.6 |
| Patient 9 | 86.9 | Patient 21 | 84.7 |
| Patient 10 | 89.2 | Patient 22 | 90 |
| Patient 11 | 89.9 | Patient 23 | 91.4 |
| Patient 12 | 91.3 | Patient 24 | 92.5 |
| | | | *Average*= 89.075<br>*Standard Deviation*=3.584 |

Two available research works were conducted on the same dataset. The result of this project work is compared with those two works. The results are compared in **Table 4.4**. From the comparison, it is found that the previous works only compared two levels of DoA, whereas this project worked on three levels of DoA. Besides, the DoA prediction accuracy of this project work is higher than the previous works.

**Table 4.4:** Comparison of the proposed work with available research works

| Name of work | Description of the work | Result |
|---|---|---|
| (Madanu, 2021) | Ensemble empirical mode decomposition and CNN-based classification method | 83.2% |
| (Rahman, 2022) | Different Band Separation and their power calculation statistically + ANN-based classification model | 86.50%±8.822 |
| Proposed Method | Parametric MUSIC Spectra + ANN | **89.01% ±3.58** |

### 4.5 Subject Independent Classification

In practical application, a subject-specific machine learning model cannot be proposed. For a practical approach, the model must be functional irrespective of the patient's age, sex, weight, etc. Therefore, at the end of this project's results, training and testing data were considered subject-independent and observed the classification results. In this approach, three different DoA of some patients' data were considered for the training, and the rest subjects' data were considered for the classification. Such results are given tabulated in **Table 4.5**. From the results of **Table 4.5**, it is found that the classification accuracy is lower than the subject-dependent approach, and it's obvious because of the inter-subject inconsistency in the EEG signal pattern for different DoA. It is also observable that with the increment of the volume of the training data, the classification accuracy is increased. Such a result is more easily perceivable from the classification results in **Figure 4.12**. In this figure, total classification accuracies are presented as a function of the number of training data and it is found that the classification accuracy is increased with the number of the training dataset.

Although the highest classification accuracy is still lower than that of the subject-dependent approach, it can predict that if the training set is very big data (at least some thousand patients' data) the prediction accuracy of the DoA level will be higher as acceptable for the clinical practice.

**Table 4.5:** Subject-independent approach of different ratios of training and testing subjects and the results of DoA prediction accuracy

| Observation No | Ratio of Training and Testing Subject | Prediction Accuracy |
|---|---|---|
| 1 | 6:18 (25% : 75%) | 32 |
| 2 | 7:17 (30% : 70%) | 38 |
| 3 | 8:16 (33% : 67%) | 31 |
| 4 | 9:15 (37.5% : 62.5%) | 42 |
| 5 | 10:14 (40% : 60%) | 45 |
| 6 | 11:13 (45% : 55%) | 50 |
| 7 | 12:12 (50% : 50%) | 48 |
| 8 | 13:11(55% : 45%) | 54 |
| 9 | 14:10 (58% : 42%) | 61 |
| 10 | 15:9 (62.5% : 37.5%) | 63 |
| 11 | 16:8 (67% : 33%) | 68 |
| 12 | 17:7 (70% : 30%) | 65 |
| 13 | 18:6 (75% : 25%) | 72 |
| 14 | 19:5 (80% : 20%) | 70 |
| 15 | 20:4 (84% : 16%) | 74 |

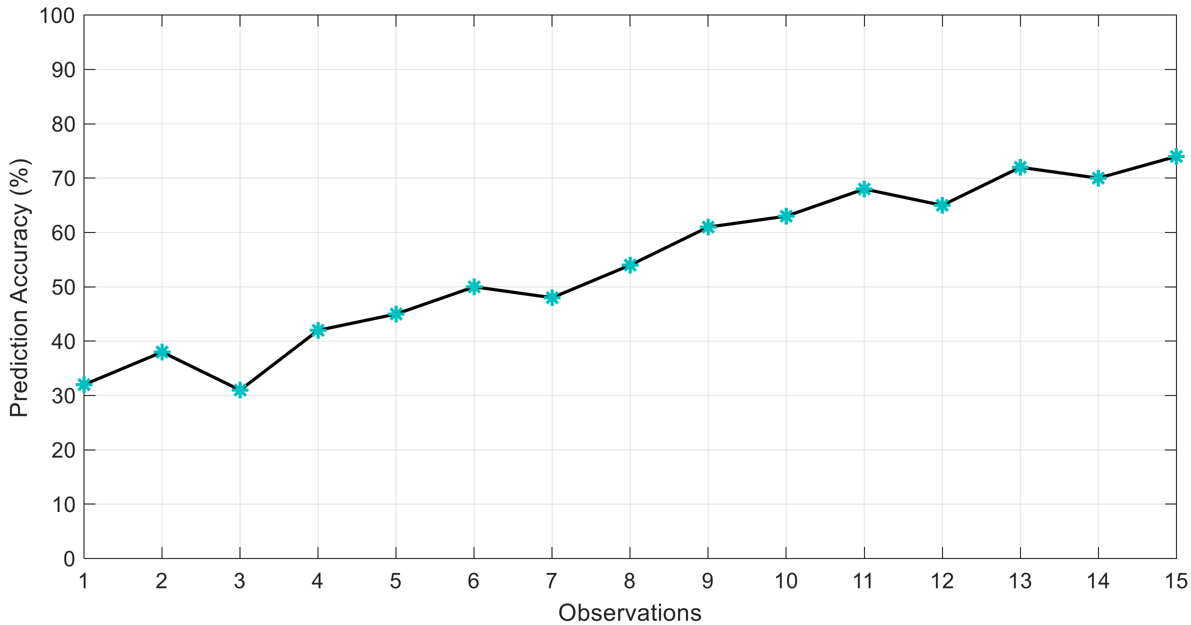


**Figure 4.12:** Subject independent prediction accuracy for the different train:test ratio as mentioned in Table 4.5

At least some hundreds to thousands of patients' data could help to develop a machine learning based predictive model for real clinical practice. This search outcome is a piece of motivation for such development and clinical practice goals. For different ages, sex, BMI, etc. the network must be more complex and fine-tuned or adjustable so that the same model can be used for different patients and different surgery.

# CHAPTER 5

# CONCLUSIONS

## 5.1 Conclusions

In this chapter, the key outcomes of this project are concluded here, briefly. The concluding remarks can be pointed out as following below:

- From 24 different patients' data the average classification accuracy was found to be 90.16 ± 2.88%.
- Among all the patients' data, for four patients (7, 9, 14, 19) the classification accuracy was found to be lower (<86%).
- The average classification accuracy was considered to be satisfactory and better than the existing research works.
- Subject independent prediction accuracy is lower than that of the subject dependent approach. The result appears to be promising as it is increasing with the volume of the training dataset

Although this research achieved some hopeful results, it has some limitations those can be improved further.

- Marginal data (Into Deep-Deep Transition and Deep-Into Awake Transition) are misclassified.
- Some null points are in the EEG data matrix for markers that affected average classification accuracy.

## 5.2 Future Perspectives

Following points could be considered as future perspective of this work:

- A visible pattern correlated to the patient sleep state can be modeled like BIS using spectral features of MUSIC algorithm.
- Except, MUSIC other parametric methods for power spectral density can be used to find the classification accuracy of the same dataset to compare the results. Also, bi-spectral features using MUSIC can be extracted to model the classifier.
- Since the EEG signal of this dataset is a long time series, for classification purpose long short term memory based recurrent neural network can be utilized.

## References


Akeju, O. W. (2014). Effects of sevoflurane and propofol on frontal electroencephalogram power and coherence. *Anesthesiology,* 121(5), 990-998.

Alsafy, I. (2022). Developing a robust model to predict depth of anesthesia from single channel EEG signal. *Physical and Engineering Sciences in Medicine,* 45(3), .793-808.

Amin, H. M. (2017). Classification of EEG signals based on pattern recognition approach. . . *Frontiers in computational neuroscience,* 11, 103.

Beibei, H. Y. (2022). Node Classification in Attributed Multiplex Networks Using Random Walk and Graph Convolutional Networks. *Frontiers in Physics,* 9(763904), 1-12.

Bertsekas, D. (2022). Newton's method for reinforcement learning and model predictive control. *Results in Control and Optimization,* 7(100121), 1-34.

Carillion, A. F. (2015). Overexpression of cyclic adenosine monophosphate effluent protein MRP4 induces an altered response to β-adrenergic stimulation in the senescent rat heart. *Anesthesiology,* 122(2), 334-342.

Cascella, M. (2016). Mechanisms underlying brain monitoring during anesthesia: limitations, possible improvements, and perspectives. *Korean journal of anesthesiology,* 69(2), 113–120.

Cascella, M. B. (2020). Awareness during emergence from anesthesia: Features and future research directions. *World journal of clinical cases,* 8(2), 245–254.

*Figshare*. (n.d.). Retrieved from https://figshare.com/articles/dataset/EEG_and_BIS_raw_data/5589841/1

Fishler, E. (2005). Estimation of the number of sources in unbalanced arrays via information theoretic criteria. *IEEE Transactions on Signal Processing,* 53(9), 3543-3553.

Frasch, M. D. (2015). Adaptive shut-down of EEG activity predicts critical acidemia in the near-term ovine fetus. *Physiological reports,* 3(7), 12435.

Goel, A. G. (2022). The role of artificial neural network and machine learning in utilizing spatial information. *Spatial Information Research*, 1-11.

Gottschalk, A. V. (2011). Is anesthesia dangerous? *Deutsches Ärzteblatt International,*, 108(27), 469.

Heggy, E. A. (2020). Intraoperative Awareness during General Anesthesia: Experience in 200 Patients in “185’s Hospital for Emergency Surgeries and Burn”. *Open Access Macedonian Journal of Medical Sciences,* 8(B), 429-434.

Höcker, J. R. (2010). Differences between bispectral index and spectral entropy during xenon anaesthesia: A comparison with propofol anaesthesia. *Anaesthesia, 14,* 26.

Hossain, S. R. (2023). Emotional State Classification from MUSIC-Based Features of Multichannel EEG Signals. *Bioengineering,* 10(1), 00.

Hutt, A. (2013). The anesthetic propofol shifts the frequency of maximum spectral power in EEG during general anesthesia: analytical insights from a linear model. *Frontiers in Computational Neuroscience,* 7, 2.

Kim, H. W. (2023). Variable three-term conjugate gradient method for training artificial neural networks. *Neural Networks,* 159, 125-136.

Kymk, M. G. (2005). Comparison of STFT and wavelet transform methods in determining epileptic seizure activity in EEG signals for real-time application. *Computers in biology and medicine,* 35(7), .603-616.

Lalitha, V. (2007). Automated detection of anesthetic depth levels using chaotic features with artificial neural networks. *Journal of medical systems,* 31, 445-452.

Likas, A. S. (2000). Training the random neural network using quasi-Newton methods. *European Journal of Operational Research,* 126(2), 331-339.

Liu, Q. M. (2018). Sample entropy analysis for the estimating depth of anaesthesia through human EEG signal at different levels of unconsciousness during surgeries. *PeerJ,* 6, 4817.

Madanu, R. R. (2021). Depth of anesthesia prediction via EEG signals using convolutional neural network and ensemble empirical mode decomposition. *Mathematical Biosciences and Engineering,* 18(5), 5047-5068.

McKeever, S. J. (2014). Sevoflurane-induced changes in infants' quantifiable electroencephalogram parameters. *Pediatric Anesthesia,* 24(7), 766-773.

Musizza, B. (2010). Monitoring the depth of anaesthesia. *Sensors,* 10(12), 10896-10935.

Nguyen, T. L. (2021). On the Training Algorithms for Artificial Neural Network in Predicting the Shear Strength of Deep Beams. (Z. Zhang, Ed.) *Complexity,* 2021(5548988), 1-18.

Poorun, R. H. (2016). Electroencephalography during general anaesthesia differs between term-born and premature-born children. *Clinical Neurophysiology,,* 127(2), 1216-1222.

Rahman, M. A. (2022). Exploring the classification performance of different EEG bands for anesthesia monitoring. *Iran Journal of Computer Science,* , 1-8.

Rani, D. (2012). Depth of general anaesthesia monitors. *Indian Journal of Anaesthesia,* 56(5), 437.

Rogobete, A. B. (2021). Multiparametric monitoring of hypnosis and nociception-antinociception balance during general anesthesia—a new era in patient safety standards and healthcare management. *Medicina,* 57(2), 132.

Shalbaf, R. B. (2015). Monitoring depth of anesthesia using combination of EEG measure and hemodynamic variables. . *Cognitive Neurodynamics, 9,* 41-51.

Shi, M., Huang, Z., Xiao, G., Xu, B., Ren, Q., & Zhao, H. (2023). Estimating the Depth of Anesthesia from EEG Signals Based on a Deep Residual Shrinkage Network. *Sensors,* 23(2), 1-16.

Shurrab, S. D. (2022). Self-supervised learning methods and applications in medical imaging analysis: a survey. *PeerJ. Computer science,* 8( e1045), 1-51.

Uhrig, L. D. (2014). Cerebral mechanisms of general anesthesia. . *Annales francaises d'anesthesie et de reanimation ,Elsevier Masson.,* 33(2), 72-82.

Vutskits, L. (2016). Lasting impact of general anaesthesia on the brain: mechanisms and relevance. *Nature Reviews Neuroscience,* 17(11), 705-717.

Xue, Y. W. (2022). A self-adaptive gradient descent search algorithm for fully-connected neural networks. *Neurocomputing,* 478(1), 70-80.

Zhang, X. R. (2001). EEG complexity as a measure of depth of anesthesia for patients. *IEEE transactions on biomedical engineering,* 48(12), .1424-1433.

# List of Publications

**Rahman, M. N.**, Ahmed, D. I., Das, P. *et al*. (2022). Exploring the classification performance of different EEG bands for anesthesia monitoring. *Iran J Comput Sci*. https://doi.org/10.1007/s42044-022-00131-8